www.sciencemag.org/content/363/6430/979/suppl/DC1

Supplementary Materials for

Impacts of historical warming on marine fisheries production

Christopher M. Free*, James T. Thorson, Malin L. Pinsky, Kiva L. Oken,
John Wiedenmann, Olaf P. Jensen

*Corresponding author. Email: cfree14@gmail.com

Published 1 March 2019, *Science* **363**, 979 (2019)
DOI: 10.1126/science.aau1758

This PDF file includes:

Materials and Methods
Supplementary Text
Figs. S1 to S30
Tables S1 to S8
References

Other Supplementary Material for this manuscript includes the following:
(available at www.sciencemag.org/content/363/6430/979/suppl/DC1)

Appendices A to G

Materials and Methods

Study design

We used a Pella-Tomlinson surplus production model (*17*) with a multiplicative temperature influence term to measure the influence of ocean warming on the productivity of 235 marine fish and invertebrate stocks in the RAM Legacy Stock Assessment Database (*19*). We estimated the sea surface temperatures (SST) experienced by each stock by mapping the boundary of the stock (i.e., the spatial domain of the stock assessment) and calculating the mean annual SST within this boundary using the COBE SST dataset (*18*). To determine whether taxonomy (order or family), geography (FAO major fishing area or ecoregion), or stock assessment method structure the SST influences, we evaluated models with hierarchical SST influence based on each of these five groups. We used Akaike Information Criterion (AIC; (*21*)) to compare models and selected the model with the lowest AIC score as the "final" model. Next, we evaluated whether the final model SST influences were additionally determined by: (1) life history traits such as growth rate, maximum age, or depth preference; (2) behavioral traits such as reproductive guild, migratory habits, or spawning behavior; (3) stock characteristics such as trend in biomass or fishing pressure; and (4) thermal experience such as mean SST, SST trend, or latitude. Lastly, we used the final model to hindcast SST-dependent maximum sustainable yield from 1930-2010 over all stocks and among ecoregions. To ensure that the estimated distribution of SST influences was not due to chance alone, we compared the final model results to results from null models using simulated SST time series designed to decouple the observed SST and productivity time series. We also explored the sensitivity of our results to using the COBE SST dataset rather than the ERSST (*53*) or HadISST (*54*) datasets and to modeling SST influence as a random rather than fixed effect.

1. Data collection

1.1 Stock selection

We analyzed the non-salmon stocks in the RAM Legacy Stock Assessment Database (RAMLDB v3.8; (*19*)) with time series of total biomass (metric tons) and catch or landings (metric tons; catch preferred) longer than 20 years after trimming years poorly informed by catch and survey data (Table S5). We identified stocks and years to trim by visually inspecting the (1) surplus production and stock-recruit relationships and (2) biomass, recruitment, and catch time series for all candidate RAMLDB stocks (Appendix A). Stocks exhibiting smooth surplus production or stock-recruit relationships over the entire time series were excluded from the analysis. Years, largely at the beginning of the time series, exhibiting flat or smooth biomass or recruitment or perfectly linear catch were excluded from the analysis. Most stocks assessed using biomass dynamics models (largely tuna and marlin stocks) were excluded from the analysis because their dynamics were strongly driven by an assumed production function. However, we included 30 stocks assessed using biomass dynamics models that were visually judged to exhibit enough process variability for consideration in the analysis. Finally, we excluded 28 stocks that prevented model convergence because they either (1) lacked periods of low exploitation and high biomass necessary to constrain carrying capacity or (2) exhibited population dynamics wildly divergent from stationary logistic population growth (Appendix B). The resulting 235 stocks represent a variety of taxa (213 bony fish, 15 crabs/shrimps/lobsters, 4 bivalves, 2 squids, 1 ray), life histories, and locations and approximately 33% of reported global catch (28 of 86 million metric tons in 2000; (*1*)).

1.2 Stock boundary delineation and SST time series

We estimated the sea surface temperatures (SST) experienced by each stock by mapping the boundary of the stock (i.e., the spatial domain of the stock assessment) and calculating the mean annual SST within this boundary using the COBE SST dataset (COBE v2; (*18*)). The COBE dataset provides monthly SST on a globally complete 1°x1° grid from 1850-present based on an interpolation of in-situ and satellite-derived SST observations. We conducted sensitivity analyses using the ERSST (*53*) and HadISST (*54*) datasets to ensure that the results were not sensitive to the choice of SST dataset (Fig. S1; Appendix C). Stock boundaries were delineated by either (1) merging the statistical/management areas used to define the assessment area; (2) digitizing the assessment area directly from the stock assessment; or (3) clipping the managing country's exclusive economic zone or the managing agency's area of competence to the geographical reference points provided in the stock assessment. In the USA and Australia, we used information on the geographic distribution of each species (i.e., essential fish habitat and modelled distribution, respectively) to further constrain stock boundaries.

2. Modeling

2.1 Overview

We modeled temperature-dependent fisheries productivity in five stages. First, we modeled productivity without a temperature effect and used this "standard" model as a benchmark for parameterizing and evaluating models with a temperature effect. Second, we extended the standard model to include a multiplicative temperature influence term and used this model to evaluate whether temperature influences fisheries productivity. Third, we added hierarchical structure to the temperature term to test whether taxonomy, geography, or stock assessment method determines temperature influences. Fourth, we developed simulated temperature time series to confirm that our results were not an artifact of model structure. Finally, we evaluated how our results and conclusions would change if the temperature influences were modeled as fixed rather than random effects. We also detail how our attempt to model dome-shaped temperature dependence by estimating an additional thermal optima parameter proved impossible because of insufficient contrast in the temperature data.

2.2 Standard surplus production model

We modeled fisheries productivity using a Pella-Tomlinson surplus production model (*17*) with first-order autocorrelation in the residuals. Observed surplus production was calculated for each stock as the net change in total biomass in the absence of harvest:

$$SP_{i,t} = B_{i,t+1} - B_{i,t} + C_{i,t} \qquad \text{Eq. 1}$$

where $SP_{i,t}$ is the surplus production for stock *i* over year *t*, $B_{i,t}$ and $B_{i,t+1}$ are the biomasses of stock *i* in years *t* and *t+1*, respectively, and $C_{i,t}$ is the catch for stock *i* removed between years *t* and *t+1*. By including the observed catch in the net change in biomass, surplus production accounts for the effect of fisheries removals on population growth (or decline). We used a Pella-Tomlinson model (*17*) because it contains a shape parameter (*p*) that allows it to replicate either the Fox ($p \rightarrow 0$) or Schaefer (p=1) production models (*55*, *56*):

$$SP_{i,t} = \frac{r_i}{p} B_{i,t} \left(1 - \left(\frac{B_{i,t}}{K_i}\right)^p\right) + \varepsilon_{i,t} \qquad \text{Eq. 2}$$

where r_i is the intrinsic rate of growth for stock *i*, K_i is the carrying capacity for stock *i*, and $\varepsilon_{i,t}$ is the residual for stock *i* in year *t*. Residuals are assumed to follow a first-order autocorrelated (AR1) process:

$$\varepsilon_{i,t} = \rho_i \varepsilon_{i,t-1} + \sqrt{1 - \rho_i^2}\,\delta_{i,t} \qquad \text{Eq. 3}$$

where ρ_i is the first-order autocorrelation coefficient for stock *i*, $\varepsilon_{i,t}$ and $\varepsilon_{i,t-1}$ are the observed residuals around the production function for stock *i* in years *t* and *t-1*, respectively, and $\delta_{i,t}$ is a normally distributed random variable representing uncorrelated errors for stock *i* in year *t*. We do not correct for the lower variance arising for $\varepsilon_{i,t}$ in the first year of data, and instead preclude doing so by estimating ρ_i with unbounded support.

We used Akaike Information Criterion (AIC; (*21*)) to compare models with shape parameters (*p*) that maximize productivity at 50% (p=1.00), 45% (p=0.55), 40% (p=0.20), and 37% (p=0.01) of carrying capacity and selected the model with the lowest AIC score as the best "standard" model. We evaluated these shape parameter values because 50% produces the symmetric Schaefer model, 40% is the meta-analytic mean for fish (*57*), and 37% is the asymptotic limit of this parameterization of the Pella-Tomlinson model.

In this model and in all the models described below, we (1) scaled biomass and production to each stock's maximum biomass to ease model fitting and (2) placed a likelihood penalty on carrying capacities greater than five times the observed maximum biomass to constrain unrealistic values. We fit all models using maximum likelihood estimation in the *TMB* package (Template Model Builder; (*58*)) in R (*59*). See Table S6 for a key to all model symbols.

2.3 Base SST-linked surplus production model

To evaluate the influence of temperature on fisheries productivity, we extended the best standard model to include a multiplicative temperature influence term:

$$SP_{i,t} = \frac{r_i}{p} B_{i,t} \left(1 - \left(\frac{B_{i,t}}{K_i}\right)^p\right) * \exp\left(SST_{i,t} * \theta_i\right) + \varepsilon_i \qquad \text{Eq. 4}$$

where $SST_{i,t}$ is the sea surface temperature for stock *i* in year *t* (centered on the mean SST for stock *i* to ease both model fitting and interpretation of the θ_i parameter) and θ_i is the influence of SST on the productivity of stock *i*. We estimated SST influences, θ_i, as random effects:

$$\theta_i \sim N(\mu_{SST}, \sigma_{SST}^2) \qquad \text{Eq. 5}$$

where μ_{SST} and σ_{SST} are the mean and standard deviation of the global distribution of SST influences (θ_i), respectively. $\theta_i < 0$ means increasing SST reduces productivity at a given biomass and $\theta_i > 0$ means increasing SST magnifies productivity at a given biomass.

We used AIC to compare models using SST averages from the COBE, ERSST, and HadISST datasets and selected the model with the lowest AIC score as the best "base" model.

2.4 Hierarchical SST-linked surplus production models

To determine whether taxonomy, geography, or stock assessment method structure SST influences, we used SST-linked surplus production models with hierarchical SST influence based on each of five groups in three categories (Table S1): (a) taxonomy (order and family); (b) geography (FAO major fishing area and marine ecoregion); and (c) stock assessment method (Table S7). Marine ecoregions were defined by intersecting Large Marine Ecosystems (LMEs; (*60*)) and High Seas Areas (HSAs; (*61*)). These models were identical to the base model except that SST influence was estimated as a nested hierarchical random effect:

$$\theta_{i,j} \sim N(\mu_{G,j}, \sigma_G^2) \qquad \text{Eq. 6}$$

where SST influences (θ_i) for stock *i* in group *j* were drawn from a normal distribution with a group-specific mean ($\mu_{G,j}$) and group-level standard deviation (σ_G). Group-specific means were drawn from a global normal distribution with mean (μ_{SST}) and standard deviation (σ_{SST}):

$$\mu_{G,j} \sim N(\mu_{SST}, \sigma_{SST}^2) \qquad \text{Eq. 7}$$

We compared the group models to the base model using AIC and judged a group to be a significant driver of SST influence if its model exhibited an AIC score more than two points lower than the base model. The best or "final" SST-linked surplus production model was identified as the model producing the lowest AIC score.

2.5 Model validation

We tested whether the final SST-linked surplus production model described population dynamics better than the standard surplus production model by competing the models using AIC. We tested whether the results of the final model were an artifact of model structure by decoupling the SST and productivity time series using three null models with different simulated SST time series exhibiting: (1) the same mean, variance, autoregressive properties, and trend as the original time series; (2) the same mean, variance, and autoregressive properties as the original time series but without a trend; and (3) the same mean and variance as the original time series but without autocorrelation or a trend (Fig. S6; Appendix D). The SST simulations were performed using the R package *forecast* (*62*). The null models were first evaluated using the true final model, which estimates first-order (AR1) autocorrelation in the residuals; however, with a weakened SST-productivity link and an AR1 process that explains a significant portion of the variability in production, the SST influences were estimated to be near zero and non-significant in all three null model scenarios. To weaken the strength of the AR1 process and better quantify the probability of measuring a significant SST influence by chance, we fixed the AR1 correlation coefficient to zero in all of the null models presented here.

2.6 Fixed effects sensitivity analysis

There are compelling arguments for estimating the influence of SST on productivity as either a fixed or random effect. On one hand, estimating SST influence as a fixed effect imposes no constraints on the magnitude and distribution of the influences and could more accurately identify influences that deviate from the patterns exhibited by other stocks in the dataset. On the other hand, estimating SST influence as a random effect could constrain poorly informed and unrealistically large influences. Thus, we evaluated the sensitivity of our results and conclusions to modeling SST influence as a random versus fixed effect. The fixed effects model was identical to the model described by Eq. 4 except that SST influence was estimated as a fixed effect. To measure the extent to which choice of modeling framework affects the results, we compared: (1) the distribution and magnitude of SST influences; (2) the importance of exploitation history, maximum age, and temperature trend in determining the influence of SST on productivity; and (3) the hindcast changes in MSY overall and among marine ecoregions.

The SST influences estimated by the random and fixed effects models were in high agreement on the direction of the influence and were generally correlated in magnitude (Fig. S9); however, and as expected, the fixed effects model estimated larger SST influences for many stocks and estimated SST influences at a higher rate of significance than the random effects model (Figs. S9 & S10). The fixed effects model estimated absolute SST influences greater than 2.0 for eight stocks (Fig. S11), one of which appears accurate (e.g., Barents Sea capelin) while the others appear spurious. The drivers of SST influence estimates were consistent between the two models: (1) chronic overfishing increases the likelihood of negative impacts of warming on productivity; (2) faster-lived fish are more sensitive, positively and negatively, to warming than slower-lived fish; and (3) the position of a population within its species-specific thermal niche determines its response to warming (Fig. S12). However, the large SST influences estimated by the fixed effects model significantly changed the magnitude of the SST-driven losses in MSY from 1930-2010. The fixed effects model documented a 21.5%

decline in MSY while the random effects model documented a 3.0% decline (Fig. S13). Hindcasts of ecoregion-scale changes in MSY were in high agreement on the direction of change and were generally correlated in magnitude (Fig. S14). However, the changes documented by the fixed effects model were larger than the random effects model with a few large departures, especially in the negative direction (Fig. S14).

We favored the random effects model because it improved estimates of SST influence for information-poor stocks, which exert considerable influence on hindcasts of SST-dependent MSY when estimated as fixed effects. The true loss in MSY of the evaluated stocks likely lies between 4.1% (final random effects model) and 21.5% (fixed effects model).

2.7 Dome-shaped temperature dependence

We attempted to fit two SST-linked surplus production models with dome-shaped temperature dependence – i.e., productivity increases as temperatures warm towards some thermal optimum but decreases once temperatures exceed this optimum – but were unable to achieve convergence with either model. The models attempt to estimate stock-specific (Eq. 8) and species-specific (Eq. 9) thermal optima, respectively:

$$SP_{i,t} = \frac{r_i}{p} B_{i,t} \left(1 - \left(\frac{B_{i,t}}{K_i}\right)^p\right) * \exp\left(-(SST_{i,t} - z_i)^2 * \theta_i\right) + \varepsilon_{i,t} \qquad \text{Eq. 8}$$

$$SP_{i,t} = \frac{r_i}{p} B_{i,t} \left(1 - \left(\frac{B_{i,t}}{K_i}\right)^p\right) * \exp\left(-(SST_{i,t} - z_j)^2 * \theta_i\right) + \varepsilon_{i,t} \qquad \text{Eq. 9}$$

where $SP_{i,t}$, $B_{i,t}$, $SST_{i,t}$, r_i, K_i, p, and $\varepsilon_{i,t}$ are the same as in the SST-linked surplus production model with monotonic SST influence (Eq. 4), z_i and z_j are the thermal optima for stock *i* and species *j*, respectively, and θ_i, the SST influence is constrained to be larger than zero (i.e., to ensure that the dome is concave down). Species-specific thermal optima do not allow local adaptation by stocks within a species but increase sample size and estimation power. We suspect that the models failed to converge because the time series are too short (39.3 yr mean) and lack sufficient SST contrast (1.6°C breadth mean) to estimate thermal optima (Fig. S15).

3. Data analysis

3.1 Drivers of temperature influence

Because the influence of SST on productivity was estimated as a random effect, our estimates of SST influence cannot be considered independent and cannot undergo post-hoc analyses using formal statistical methods (i.e., formal hypothesis testing requires including explanatory variables inside the model, as we did with taxonomy and geography). Therefore, we graphically evaluated whether SST influence is determined by: (1) life history traits such as growth rate, maximum age, or depth preference; (2) behavioral traits such as reproductive guild, migratory habits, or spawning behavior; (3) stock characteristics such as trend in biomass or fishing pressure; and (4) thermal experience such as mean SST, SST trend, or latitude. A list of evaluated explanatory variables and their sources is provided in Table S3. We could not include these drivers inside the model, as we did with taxonomy and geography, due to missing data for many of the evaluated explanatory variables (Table S3).

3.2 Hindcasting maximum sustainable yield

We used the final model's estimates of p, r_i, K_i, and θ_i to hindcast SST-dependent maximum sustainable yield (MSY) from 1930-2010 (Appendices E-G). We expanded the equation for MSY from the Pella-Tomlinson surplus production model:

$$MSY = \frac{r * k}{(p+1)^{(p+1)/p}} \quad \text{Eq. 10}$$

to include the SST influence term and calculated MSY for stock i in year t as:

$$MSY_{i,t} = \frac{\left[(\exp(\hat{\theta}_i * \overline{SST}_{i,t}) * r_i\right]_i * k_i}{(p+1)^{(p+1)/p}} \quad \text{Eq. 11}$$

where $\overline{SST}_{i,t}$ is $SST_{i,t}$ centered on the mean of the SST data used in model fitting and $\hat{\theta}_i$ is randomly drawn from a multivariate normal distribution described by the mean θ_i estimate and the θ_i covariance matrix. We bootstrapped 10,000 MSY hindcasts for each stock to generate median MSY trends and confidence intervals. We assessed changes in MSY over the hindcast period using (1) Thiel-Sen regression slopes and (2) percent change in mean MSY from 1930-39 to 2001-2010. Theil-Sen regression, a form of robust regression, identifies the median slope of lines through all possible point pairs and is insensitive to outliers and endpoints in short time series. We limited the hindcast from 1930-2010 to minimize the extrapolation of MSY predictions to temperatures cooler or warmer than those used in model fitting (Fig. S24) and explored the sensitivity of measures of MSY change to the selection of hindcast window (Fig. S25).

3.3 Extrapolating vulnerability of global fish populations

We identified global fish populations in the FAO landings database (*1*) that are likely to be vulnerable to ocean warming as populations that (1) are overfished; (2) have experienced warming; and (3) are located at the warm end of their species-specific thermal niche.

We analyzed the 1,740 FAO fish stocks (FAO area-country-species triples) meeting the following criteria: marine wild capture fisheries for finfish and invertebrates with taxonomic identification resolved to the species-level and with catch time series ≥20 yrs and ≥250 mt of median annual catch after trimming years of zero catch from the beginning of the time series. We excluded: (1) stocks of invertebrate species that frequently lack the life history data required for the catch-only stock assessment model used to determine stock status (e.g., barnacles, corals, sea cucumbers, sea urchins, starfish, sponges); (2) stocks of highly migratory species whose population dynamics cannot be described by catch within a single country's exclusive economic zone (e.g., tuna, marlin, swordfish); and (3) stocks targeted by a distant water fleet whose catch time series are unlikely to be representative of total removals from that population (i.e., stocks whose FAO area and EEZ don't overlap were excluded).

We determined stock status using catch-MSY (*63*), the best performing individual catch-only stock assessment method (*64*). Catch-MSY is a stock reduction analysis that reconstructs historical abundance by simulating biomass trajectories that could produce the observed catch time series given priors on initial and final year depletion and stock dynamics such as carrying capacity, *K*, and intrinsic growth rate, *r*. The method establishes priors for *r* based on population resilience (see below), *K* based on maximum catch (e.g., between C_{max} and $100*C_{max}$), and initial and final year depletion based on the ratio of initial and final year catch to the maximum catch. It then estimates "viable" pairs of *r* and *K* (i.e., pairs that do not allow the stock to collapse or exceed carrying capacity), generates biomass trends for each pair, and estimates B/B_{MSY} as the median trend. We calculated the mean B/B_{MSY} of each population over the last 25 years (1991-2015) and defined overfished as $B/B_{MSY} < 0.5$. The model converged for 1530 of the 1740 stocks.

In addition to a catch time series, cMSY requires an estimate of population resilience (i.e., the ability of a population to recover from disturbance) to establish a prior for the intrinsic growth rate. We derived resilience estimates for all species using a combination of FishBase (*65*), SeaLifeBase (*66*), and FishLife (*67*) life history information. We used the *rfishbase* package (*68*) to download Von Bertalanffy growth parameters, maximum size, and vulnerability and resilience from FishBase (FB, for finfish) and SeaLifeBase (SLB, for invertebrates). We used the *FishLife* package to estimate the Von Bertalanffy growth parameters for all finfish species. *FishLife* uses a multivariate model trained on FishBase to predict eight life history traits for >32,000 fish. We classified species into resilience categories (Table S8) using, in order of preference, resilience values: (1) reported on FB/SLB; (2) derived from the FishLife Von Bertalanffy growth parameter; (3) derived from the FB/SLB Von Bertalanffy growth parameter; (4) derived from the FB/SLB vulnerability metric; (5) derived from the FB/SLB Von Bertalanffy maximum age; (6) derived from the genus mode; or (7) derived from the family mode.

We estimated the temperature experienced by each population using the COBE sea surface temperature dataset (*18*) and the spatial boundary of the population (i.e., the intersection of the FAO region and exclusive economic zone). We calculated the mean annual temperature and the trend in annual temperature over the last 25 years (1991-2015). We estimated the position of each population in its species-specific thermal niche as the percentile of the population's mean temperature experience relative to the temperature experiences of other conspecific populations. We identified populations above the 80th percentile as being at the warm end of their species-specific thermal niche.

Supplementary Text

Stock assessment models and treating output as "data"

Overview of the assessment model types included in our analysis

Stock assessments are population models that combine different sources of information (catch, relative abundance, and life history) to estimate population size and harvest rates over time, as well as the reference points used in management. Different assessment models are used based on the available data for a stock. The four categories of commonly used assessment model types in our analysis were (Table S7): biomass dynamic models (BDM), virtual population analyses (VPA), statistical-catch-at-age models (SCAA), and integrated analyses (IA).

BDMs track changes in total biomass from one year to the next, ignoring size- or age-structure in the population. Changes in biomass are due to the observed catch and estimated surplus production in a given year (assumed to be a function of biomass in that year). BDMs require annual estimates of total catch and relative abundance (CPUE, catch-per-unit-effort) to estimate the parameters controlling production and biomass over time.

VPA and SCAA models, on the other hand, assume that population dynamics are age-structured, with recruitment events producing different-sized cohorts in the population over time. VPAs use observed catch-at-age (assumed known without error) and an assumed natural mortality rate (*M*) to reconstruct historical cohort abundance using a backwards tuning procedure (tuned to available CPUE data), and total biomass each year is estimated using the estimated numerical abundance of each cohort in that year times an assumed weight-at-age. In contrast, SCAA models are forward projecting, and allow for catch data to be uncertain. Annual cohort sizes and other parameters are estimated statistically using maximum likelihood or Bayesian approaches and fit to the available catch-at-age and CPUE information. Total biomass is estimated using the estimated numerical abundance and an assumed weight-at-age. Like VPAs, SCAA models often use an assumed *M* (either fixed over time or ages, or both), although *M* can sometimes be an estimated parameter.

IA is a general assessment approach that aims to incorporate all the available data in as raw a form as possible into a single analysis via joint likelihood functions (*69*). The vast majority of assessments classified as IA in Table S7 (49 of 57) use the age-based Stock-Synthesis program (*70*), and are analogous to SCAA models in how annual estimates of biomass are produced. A key distinction between these IA models and those labeled SCAA here is that many of the inputs assumed fixed in SCAA may be estimated within the IA model, accounting for uncertainty in these quantities (e.g., weight-at-age, ageing error in catch-at-age data, etc.).

Problems with and recommendations for using stock assessment output as data

Maunder and Punt (*69*) outline five problems with using model output as data: (1) loss of information when converting data to model output; (2) inconsistent assumptions between the meta-analysis model and stock assessment model; (3) challenges in identifying a statistical likelihood for model output when treated as data; (4) difficulties in representing precision of model output (i.e., due to covariance or non-normal distribution of model estimates); and (5) reduced ability to diagnose goodness of fit for the meta-analysis model.

Thorson et al. (*47*) provide six recommendations for conducting fisheries meta-analyses: **(R1)** choose appropriate model complexity and sample size; **(R2)** use multiple lines of evidence to support a hypothesis or interpretation; **(R3)** consider alternative hypotheses; **(R4)** strive for single-stage meta-analysis; **(R5)** account for experimental, parametric, and functional variability; and **(R6)** identify the desired type(s) of inference and proceed accordingly.

Brooks and Deroba (*46*) suggest that post-hoc analyses that use model output as data frequently fail to account for the assumptions, uncertainties, and biases of the original assessment models. They provide the following five recommendations: **(R7)** avoid using model output as data; **(R8)** collaborate with lead assessment scientists; **(R9)** conduct sensitivity analyses; **(R10)** use errors-in-variables methods; and **(R11)** use cross-validation methods.

How we addressed these challenges

We mitigated the problems associated with using stock assessment output as data in fisheries meta-analyses by: **(R1)** using a simple model given our low sample size (235 time series); **(R2)** using multiple lines of evidence to corroborate our results including repeating the analysis with multiple SST datasets, parameterizations, modeling frameworks, and metrics of MSY change; **(R6)** clearly stating our intent to make global-, group- (e.g., family, ecoregion), and individual-scale (i.e., stock) inferences about the effect of SST on productivity. We also addressed the assumptions, uncertainties, and biases in using stock assessment output as data by trimming or removing time series produced with strict assumptions, removing trimmed assessments with short time series (<20 yr), using a mixed-effects model to share information between stocks and constrain poorly informed estimates, and explicitly examining the influence of assessment method on our results. The results were not affected by stock assessment method and were not sensitive to SST dataset, model parameterization, or metric of MSY change. Following **(R1)**, we recommend that future region-specific studies validate our results using meta-analytic models that leverage the availability of higher resolution data at smaller spatial scales.

We were unable to: (**R3)** consider alternative environmental drivers of fisheries productivity given the lack of historic, globally complete data on environmental variables besides SST; **(R4/R7)** use a single-stage meta-analysis given the global-intent of our study and the lack of unprocessed data (i.e., survey data) at the global-scale; **(R5/R10)** incorporate reported measures of uncertainty given that this data is not included in the RAMLDB and not reported in a consistent manner in stock assessments; **(R8)** collaborate with lead assessment scientists for all 235 assessments represented in our study; **(R9)** conduct sensitivity analyses using alternative biomass estimates or confidence intervals for biomass estimates given that this data is not included in the RAMLDB and not reported in a consistent manner in stock assessments; or **(R11)** use cross-validation methods to quantify uncertainty since withholding a testing dataset truncates our already short time series (40 yr mean). We know of only one published meta-analysis that used a single-stage analysis to estimate stock-recruit relationships for multiple populations simultaneously (*71*) and this analysis involved fewer than ten species.

Supplemental Figures

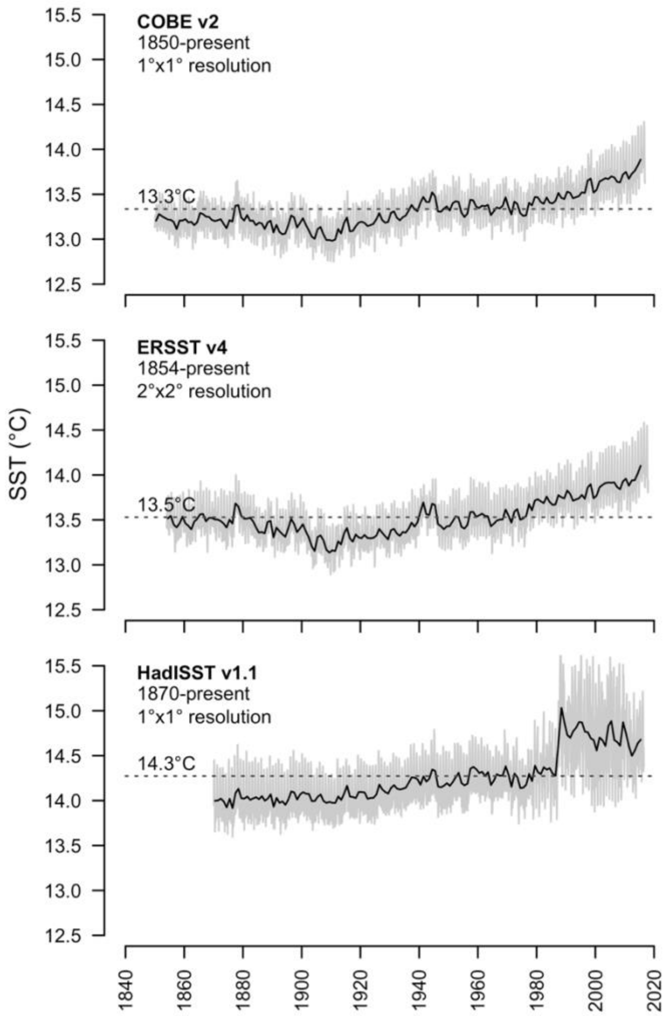

Fig. S1. Mean global SST based on the COBE v2, ERSST v4, and HadISST v.1.1 datasets. Gray lines show monthly means and black lines show annual means. Horizontal dashed lines show mean ocean temperature from 1880-present. The discontinuity in the HadISST dataset in the 1980s is likely due to problems at the poles and dateline and problems with the bias correction algorithms and compromises the usefulness of the dataset for our purposes.

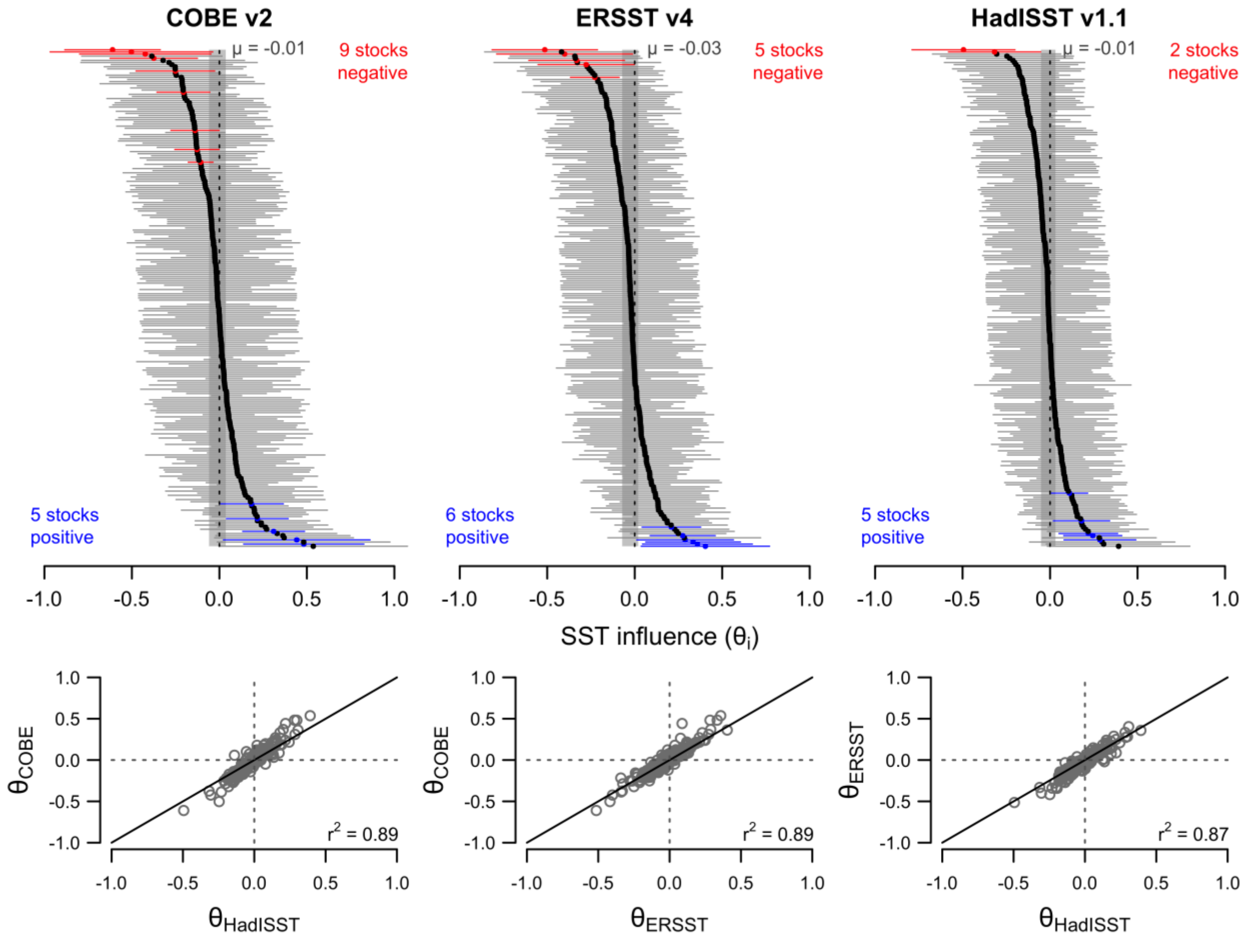

Fig. S2. <u>Comparison of SST influence estimates from SST-linked surplus production models using the COBE v2, ERSST v4, and HadISST v1.1 datasets.</u> In the top panels, points show mean estimates and error bars show 95% confidence intervals. Significant positive and negative SST influences are shown in blue and red, respectively. The shaded grey column indicates the 95% confidence interval for the global mean of the SST influences. In the bottom panels, the diagonal line is the one-to-one line for pairwise comparisons of SST influence estimates from models using each SST dataset.

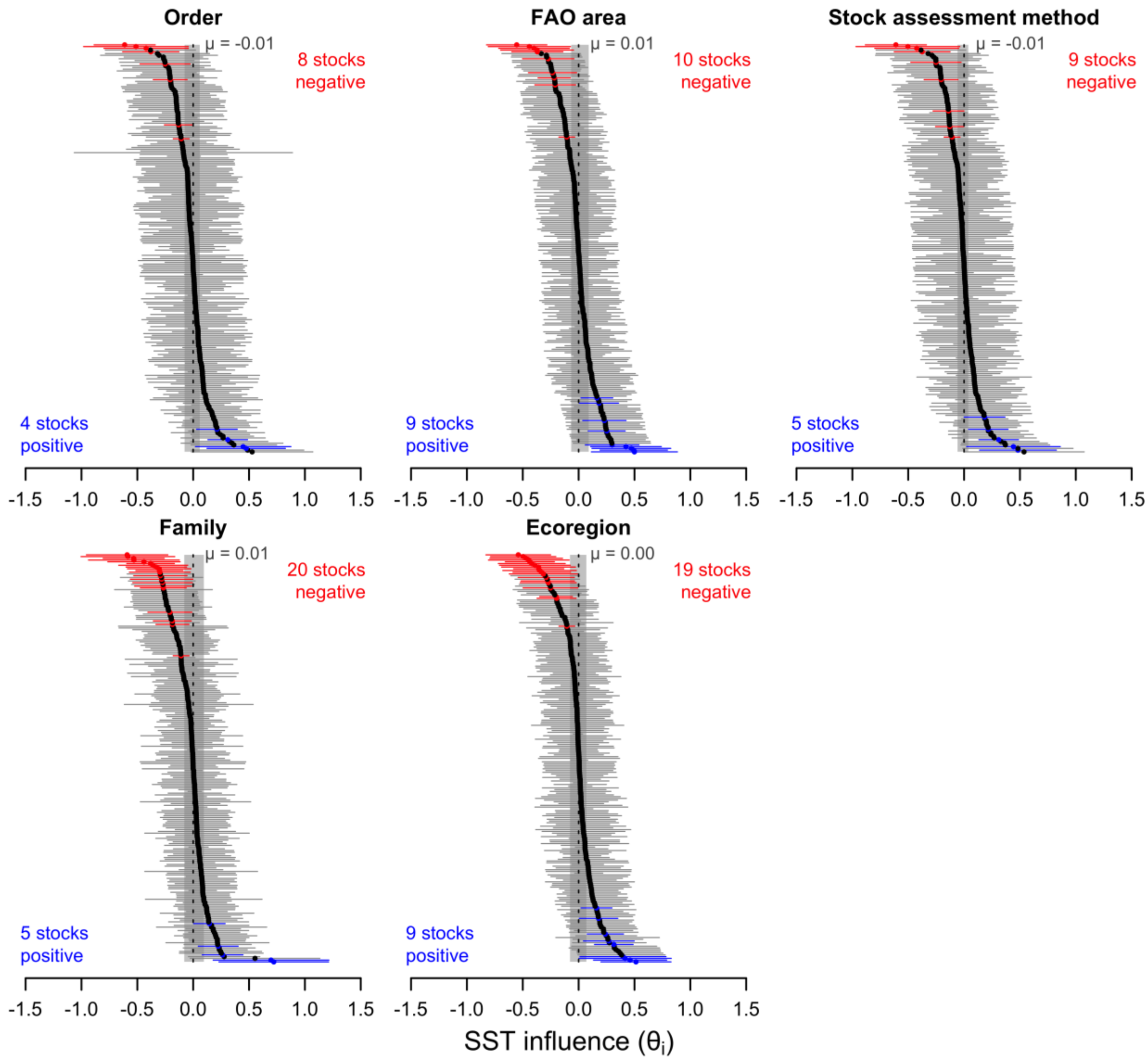

Fig. S3. <u>Distribution of SST influences estimated by SST-linked surplus production models with hierarchy on SST influence.</u> Hierarchical models are structured by (A) taxonomic order and (B) taxonomic family, (C) FAO major fishing area, (D) marine ecoregion, and (E) stock assessment method. Points show mean estimates and error bars show 95% confidence intervals. Significant positive and negative SST influences are shown in blue and red, respectively. The shaded grey column indicates the 95% confidence interval for the global mean of the SST influences.

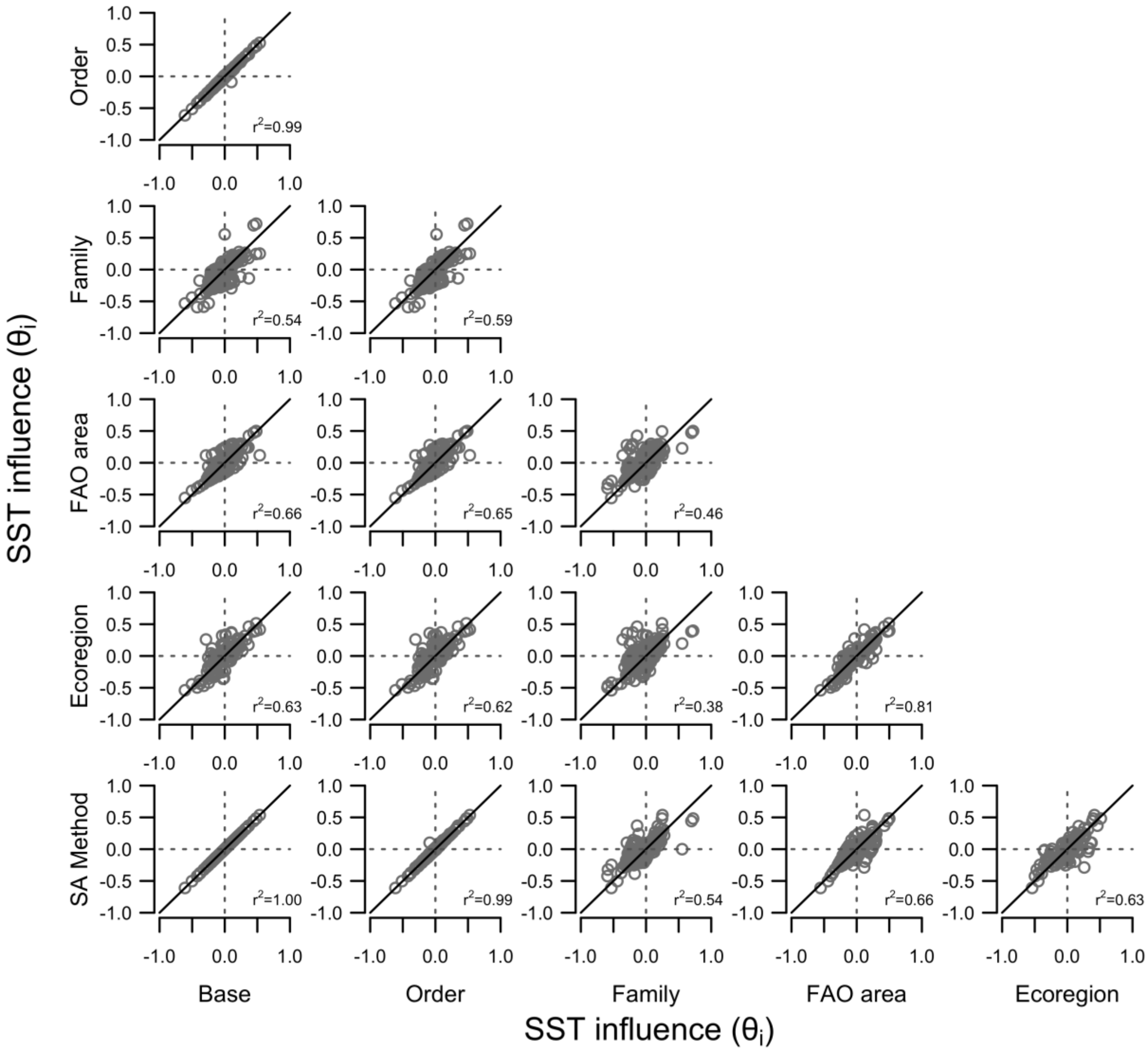

Fig. S4. <u>Correlation between SST influences estimated by the base model and five hierarchical models</u>. Hierarchical models are organized by taxonomy (order/family), geography (FAO area/marine ecoregion), or stock assessment method. Diagonal line is the one-to-one line.

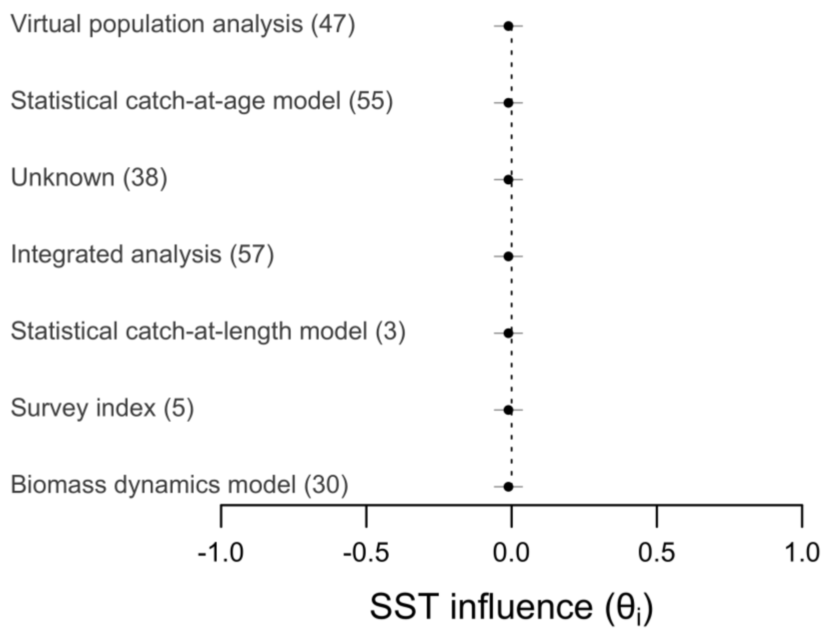

Fig. S5. **Mean of the SST influence distributions for stock assessment methods in the SST-linked surplus production model with hierarchy on SST influence by stock assessment method.** Points show mean estimates and error bars show 95% confidence intervals. None of the SST influence means were significantly different from zero and the model gained less support than the base model (see Table S1).

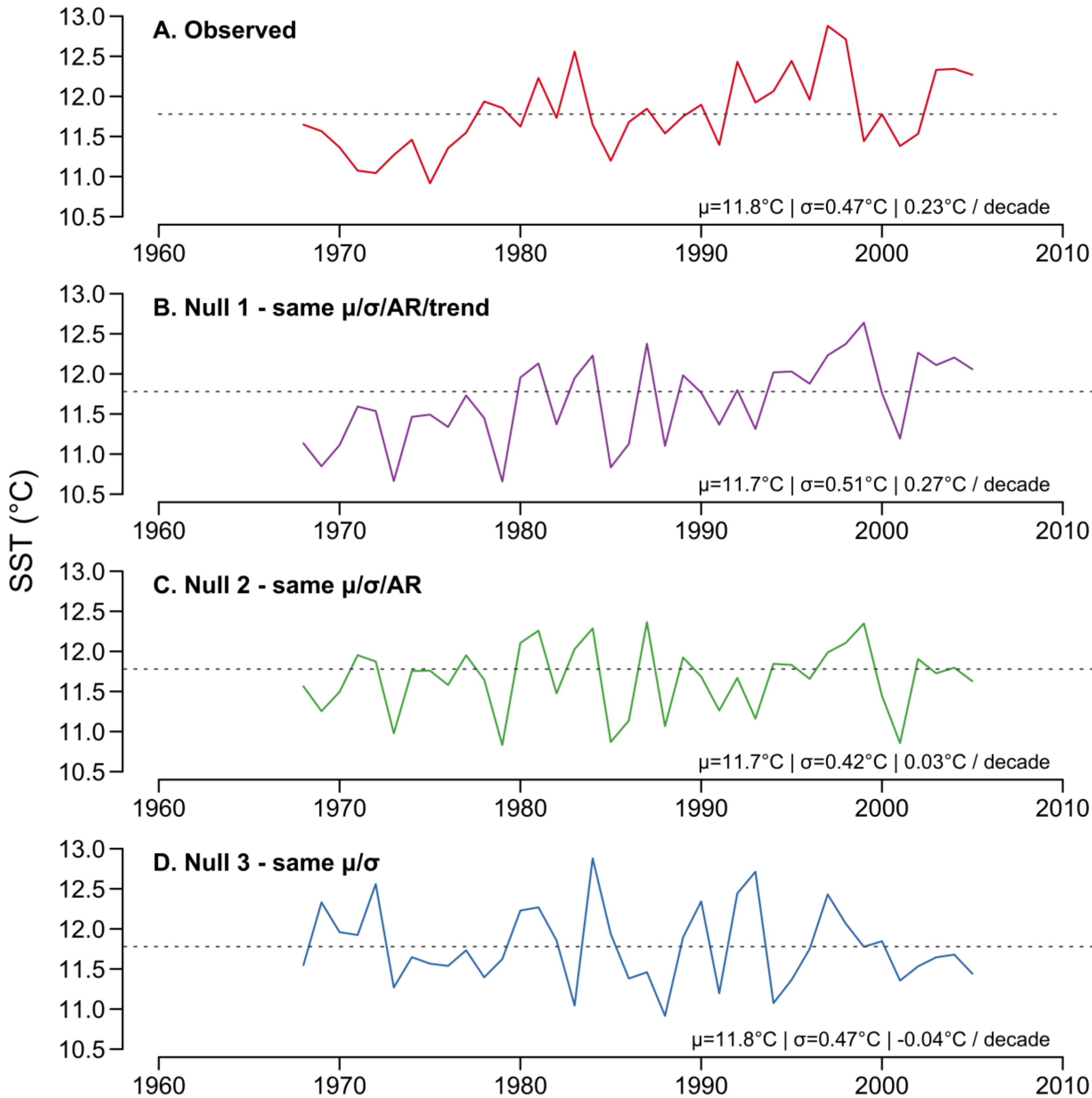

Fig. S6. <u>Example (A) observed and (B-D) simulated SST time series (US West Coast, black rockfish).</u> The simulated SST time series were used in the three null models.

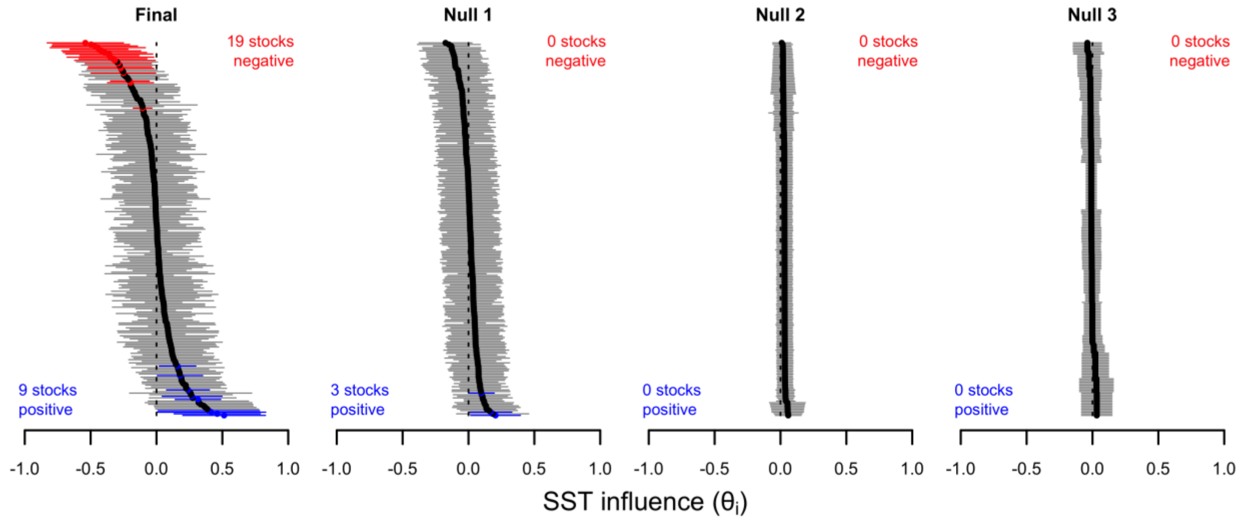

Fig. S7. <u>Distribution of SST influences estimated by the final model and three null models.</u> Points show mean estimates and error bars show 95% confidence intervals. Significant positive and negative SST influences are shown in blue and red, respectively.

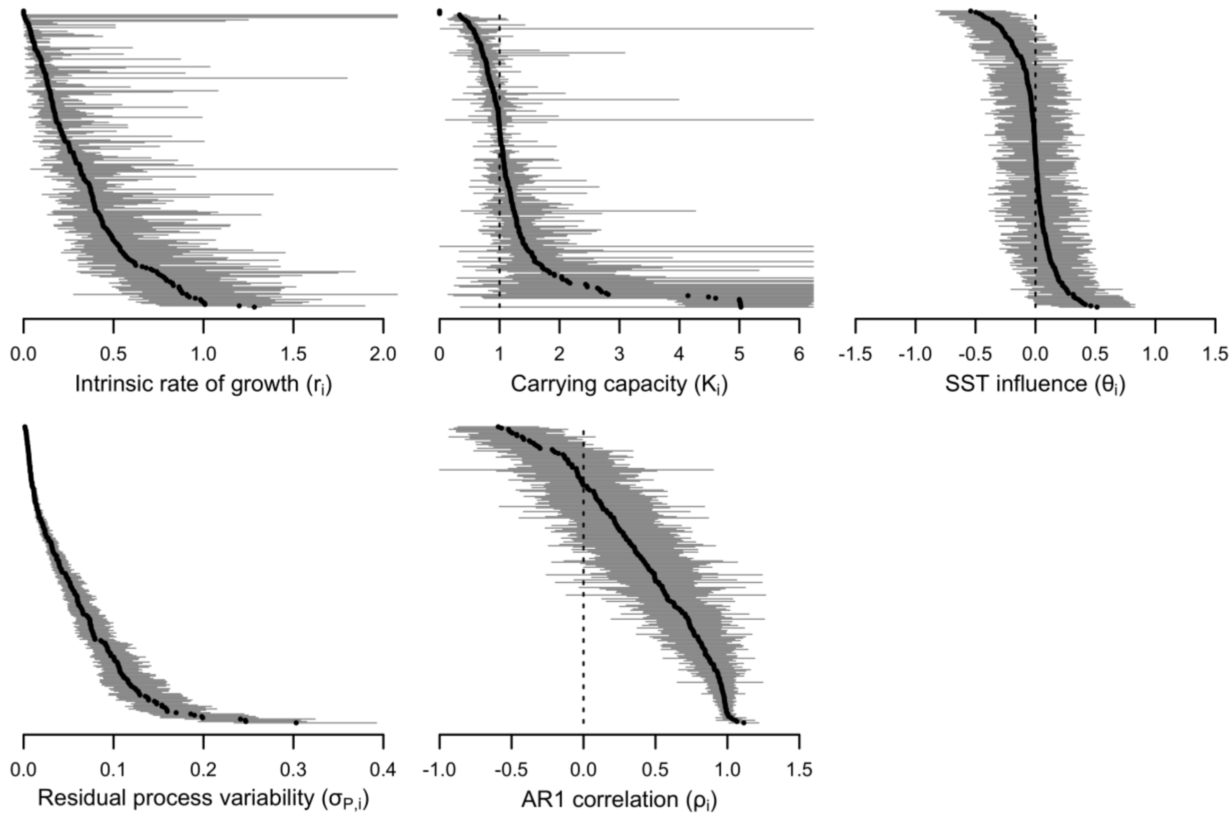

Fig. S8. **<u>Distribution of intrinsic rate of growth (r_i), carrying capacity (K_i), SST influence (θ_i), residual process variability ($\sigma_{P,i}$), and first-order (AR1) autocorrelation coefficient (ρ_i) estimates from the final model.</u>** Points show mean estimates and lines show 95% confidence intervals. Carrying capacity is a multiple of the maximum observed biomass (e.g., a carrying capacity of 1, shown by the vertical dotted line, means that the carrying capacity is equivalent to the maximum observed biomass).

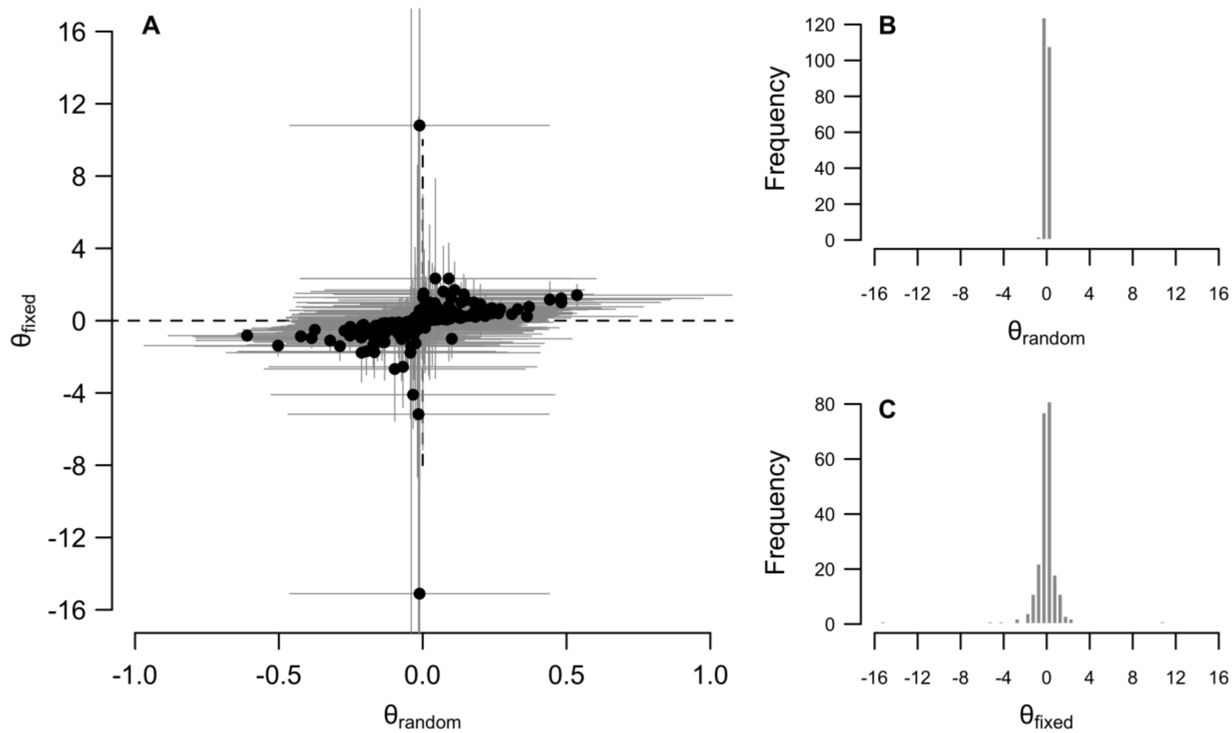

Fig. S9. **<u>Comparison of SST influences estimated by the fixed and random effects models.</u>** Plots show (A) correlation between the random and fixed effects estimates and histograms of the (B) random and (C) fixed effects estimates.

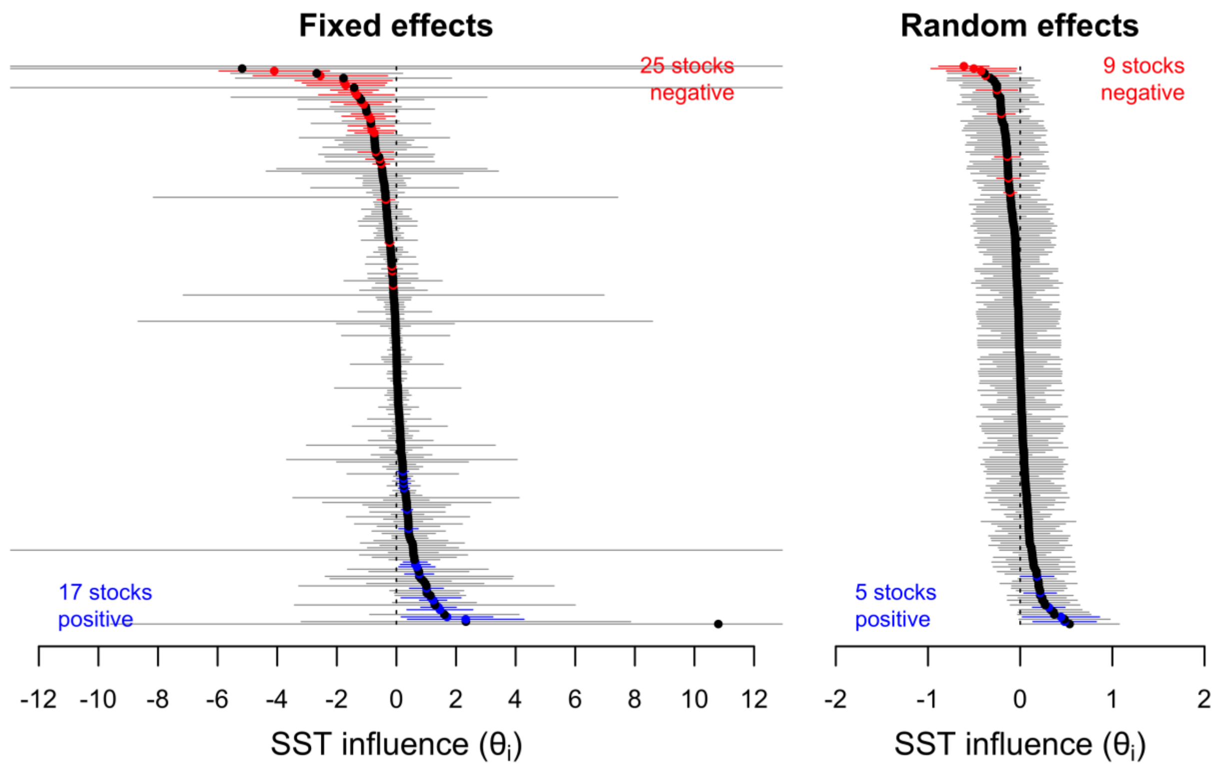

Fig. S10. <u>**Distribution of SST influences estimated by the fixed and random effects models.**</u> Points show mean estimates and error bars show 95% confidence intervals. Significant positive and negative SST influences are shown in blue and red, respectively.

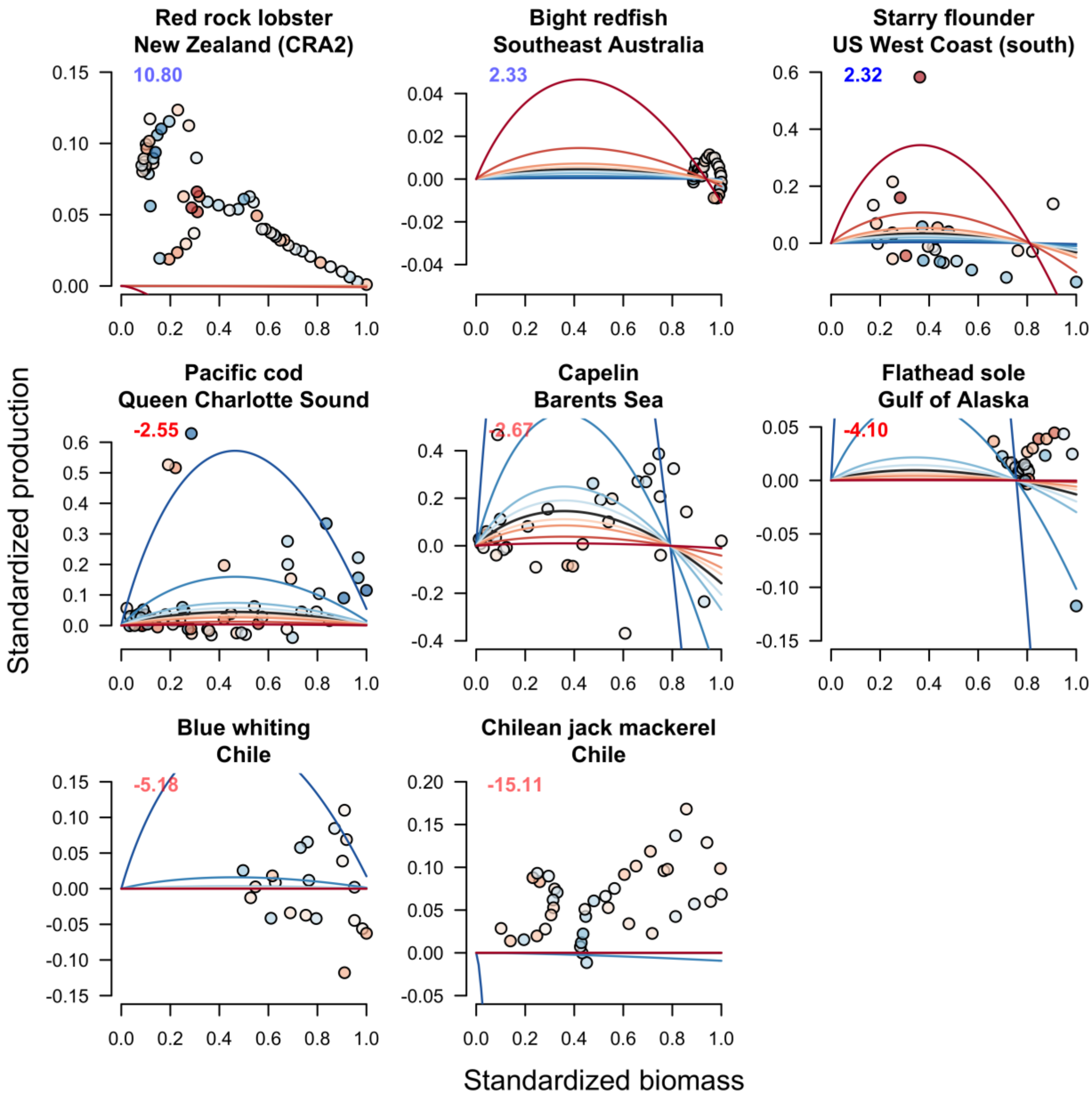

Fig. S11. <u>**Inspection of the stocks exhibiting SST influence estimates greater than 2.0.**</u> Blue points represent cooler than average years and red points represent warmer than average years. Black lines show the surplus production curves at each stock's average temperature. Blue and red lines show surplus production curves at temperatures progressively cooler and warmer than the average, respectively. Stocks with positive SST influences are more productive at warmer temperatures (red curves on top) and stocks with negative SST influences are more productive at cooler temperatures (blue curves on top). SST influences (θ_i) are shown in the top-left corner of each plot and are colored to indicate the direction and significance of the SST influence (blue=positive, red=negative, bold=significant).

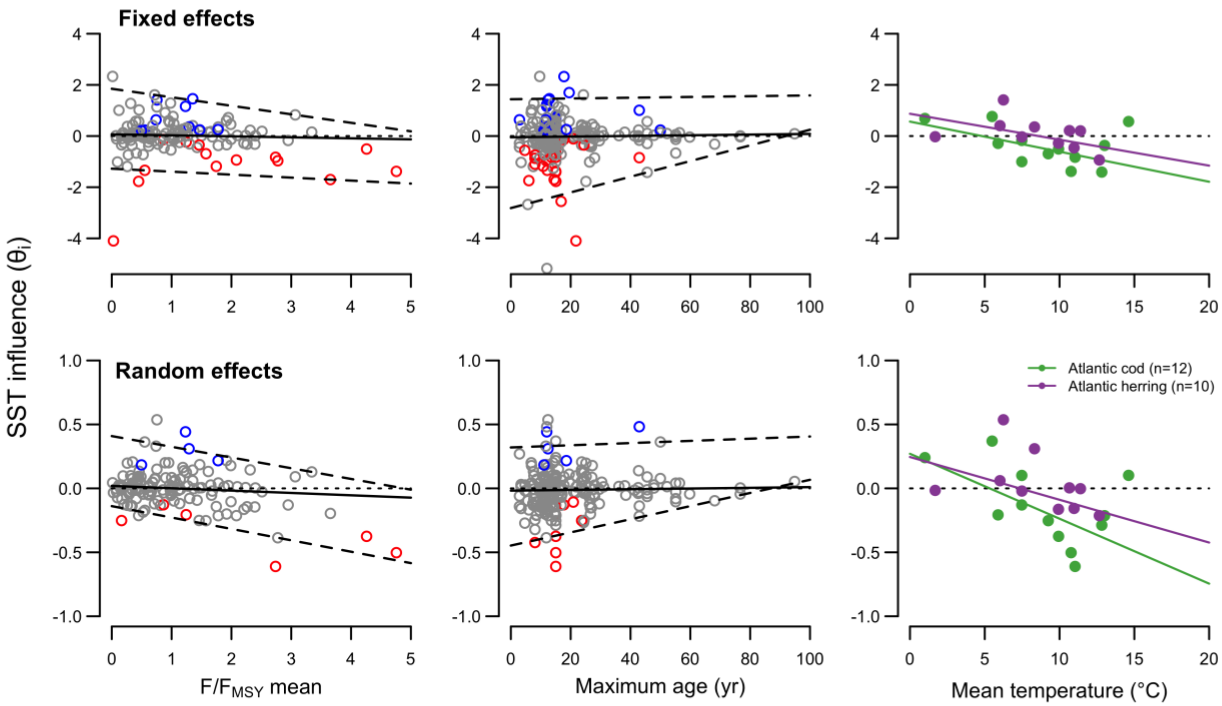

Fig. S12. <u>SST influence as a function of (A) exploitation history, (B) maximum age, and (C) position of a population in its species-specific thermal niche.</u> Panel (A) shows more and larger negative influences of warming for populations with histories of overfishing. Points represent individual populations and are colored by significance (blue=positive, red=negative, grey=non-significant). Solid lines show the 50th percentile quantile regression fit and dashed lines show the 2.5% and 97.5% quantile regression fits. F/F$_{MSY}$ is the ratio of fishing mortality (F) to the fishing mortality that produces maximum sustainable yield (F$_{MSY}$): values greater than one indicate overfishing. Panel (B) shows larger and more significant influences of temperature for populations of species with faster life histories (i.e., shorter lifespan). Points and lines as in Panel (A). Panel (C) shows increasingly negative influences for populations at the warm end of their thermal niche for the two species with ≥10 populations. Lines show Theil-Sen regression fits. Theil-Sen regression, a form of robust regression, identifies the median slope of lines through all possible point pairs and is insensitive to outliers and endpoints in small datasets.

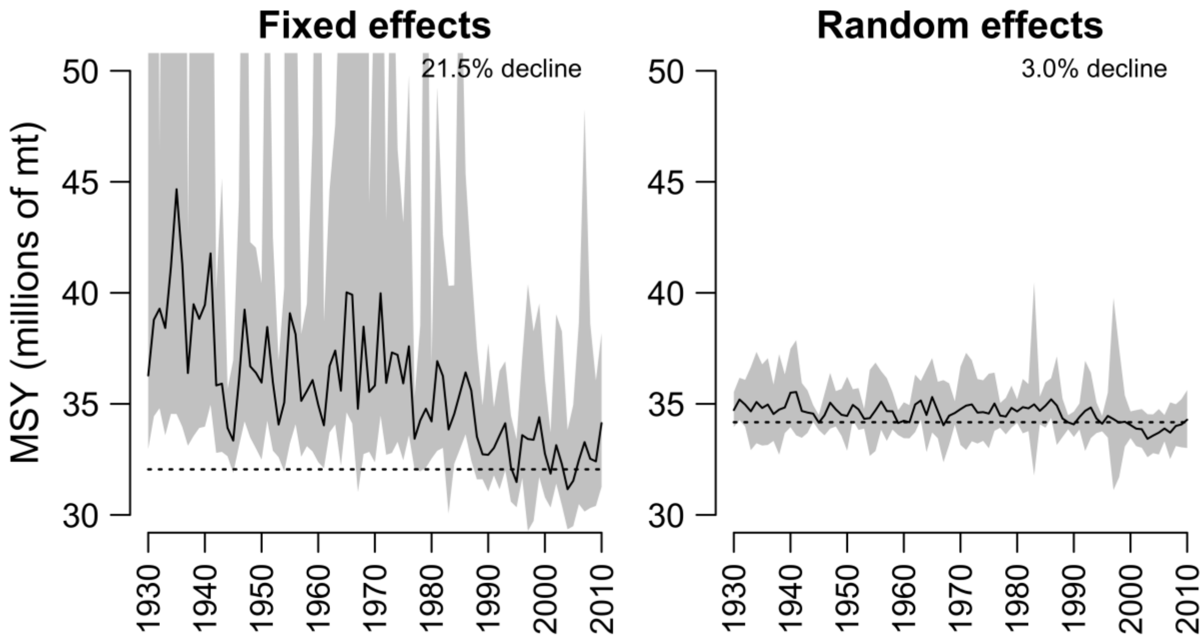

Fig. S13. Hindcast of SST-dependent maximum sustainable yield (MSY, mt=metric tons) using the fixed and random effects models. Solid lines indicate the median MSY estimates, shading indicates the 95% confidence intervals, and horizontal dashed lines indicate MSY at average temperature. Percent decline from 1930-39 to 2001-10 is shown in the top-right corner.

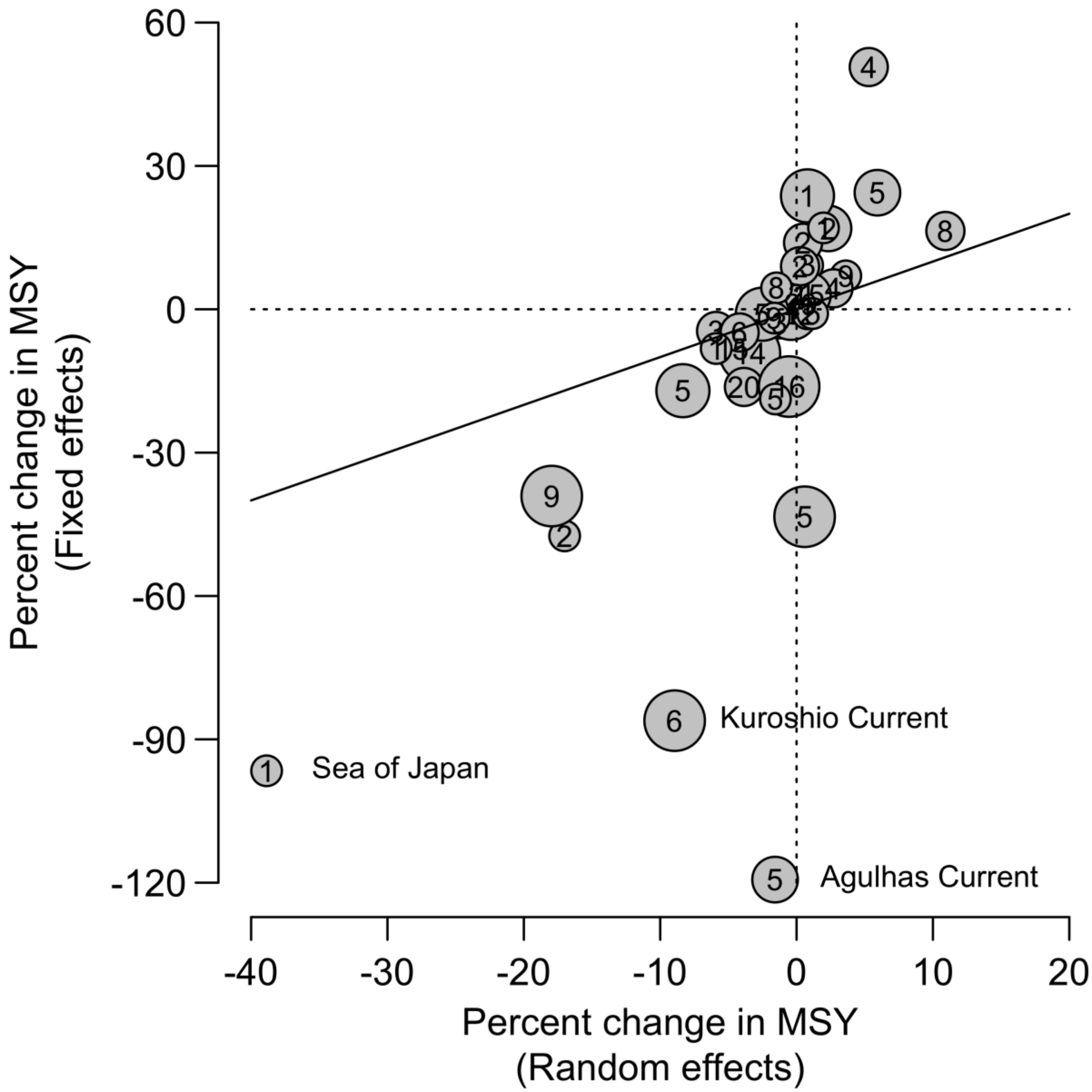

Fig. S14. **<u>Percent change in mean maximum sustainable yield (MSY) from 1930-39 to 2001-10 by ecoregion predicted by the fixed versus random effects models.</u>** Points are scaled to the MSY of the ecoregion and the number of stocks in the ecoregion is shown inside each point. The solid line indicates the one-to-one line.

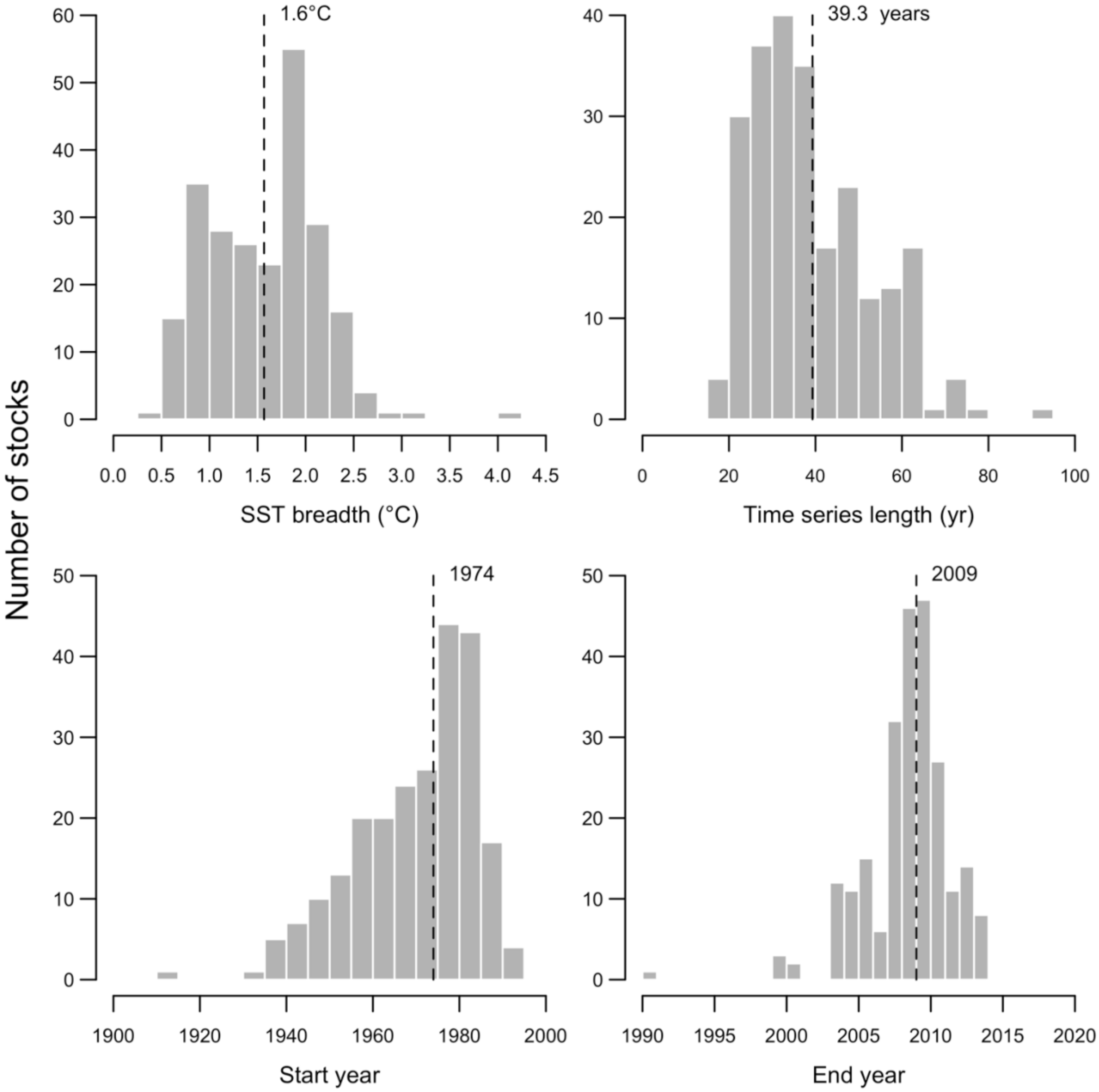

Fig. S15. <u>Histograms showing (A) breadth of SST experience, (B) length of time series, and the (C) start and (D) end year of time series for stocks used in the analysis.</u> Mean values are indicated by the vertical dashed line (median values shown for start and end years).

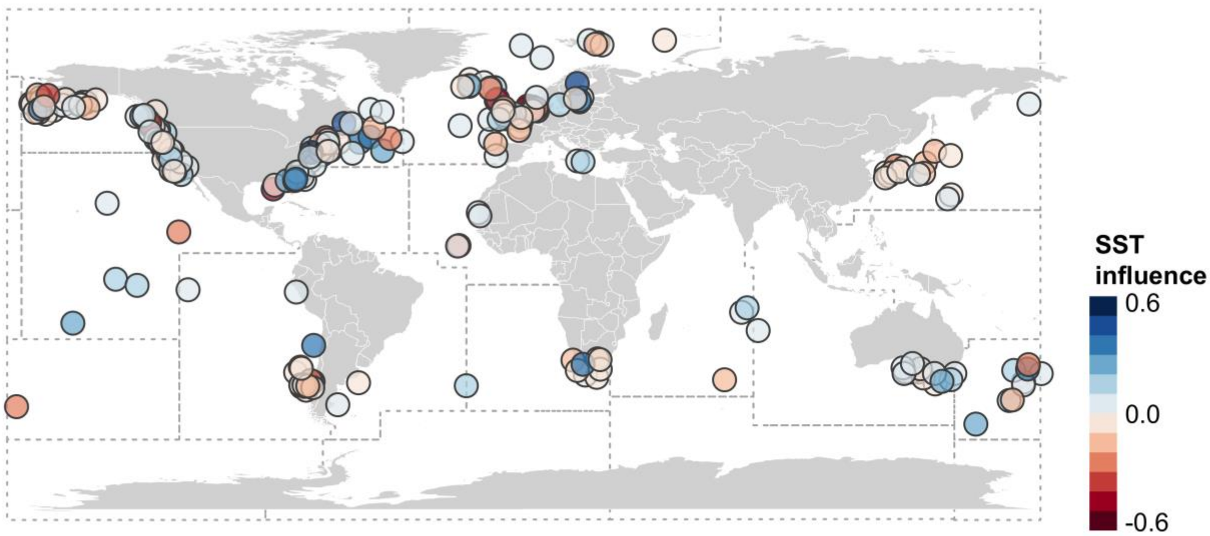

Fig. S16. **Map showing the global distribution of SST influences.** Points were jittered to expose overlapping stock centroids. Dashed lines indicate FAO major fishing areas.

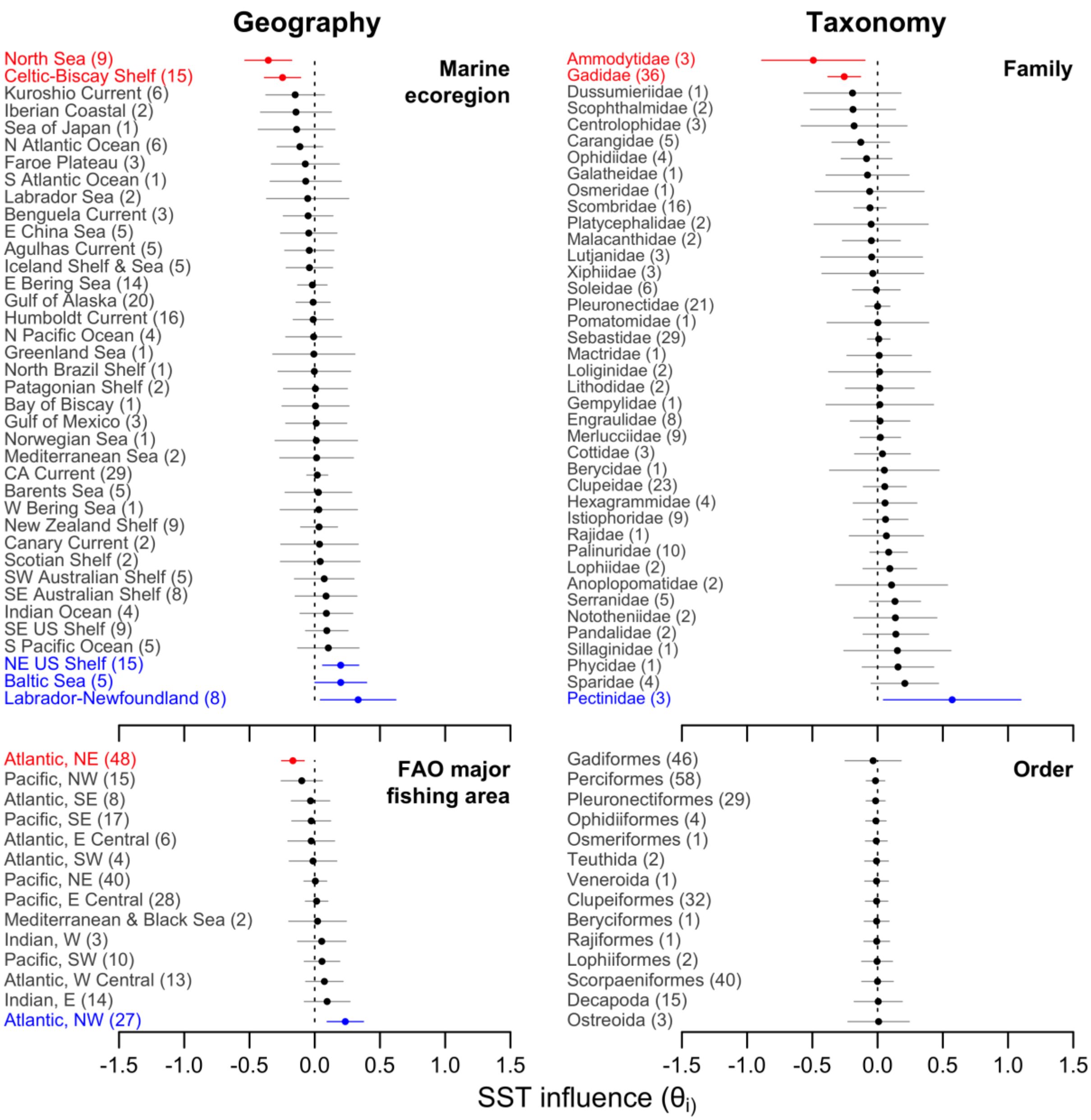

Fig. S17. <u>Mean of the SST influence distributions for geographic or taxonomic groups in models with hierarchy on SST influence.</u> Hierarchical models are structured by (A) marine ecoregion, (B) FAO major fishing area, (C) taxonomic family, and (D) taxonomic order. Points show mean estimates and error bars show 95% confidence intervals. Significant positive and negative SST influences are shown in blue and red, respectively. All but the taxonomic order model had more support than the base model.

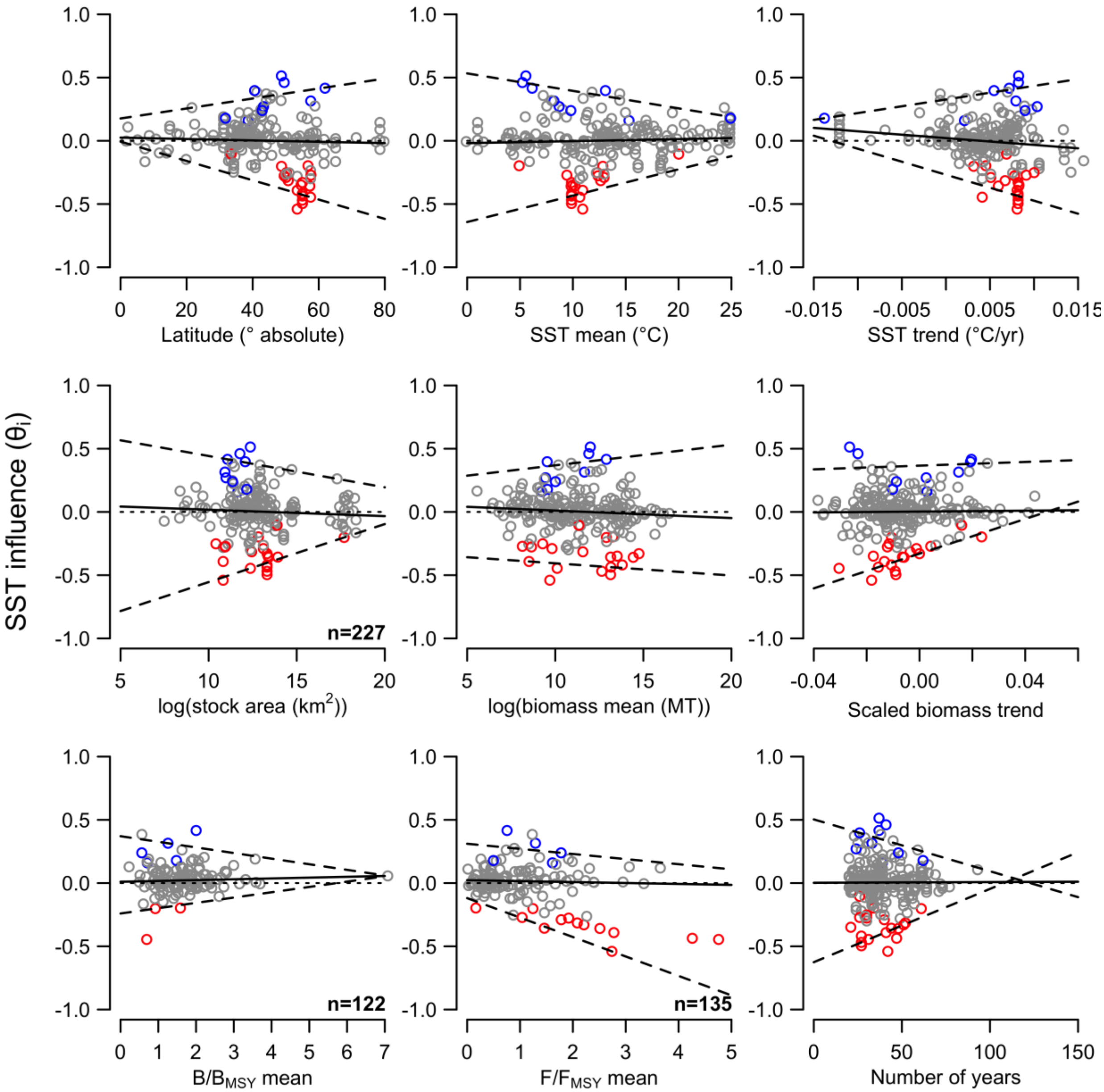

Fig. S18. <u>SST influence as a function of nine stock characteristics</u>. SST influences are colored by significance (blue=positive, red=negative, grey=non-significant). Solid lines show the 50th percentile quantile regression fit and dashed lines show the 2.5% and 97.5% quantile regression fits. Sample size is shown in the bottom-right corner if data were not available for all 235 stocks.

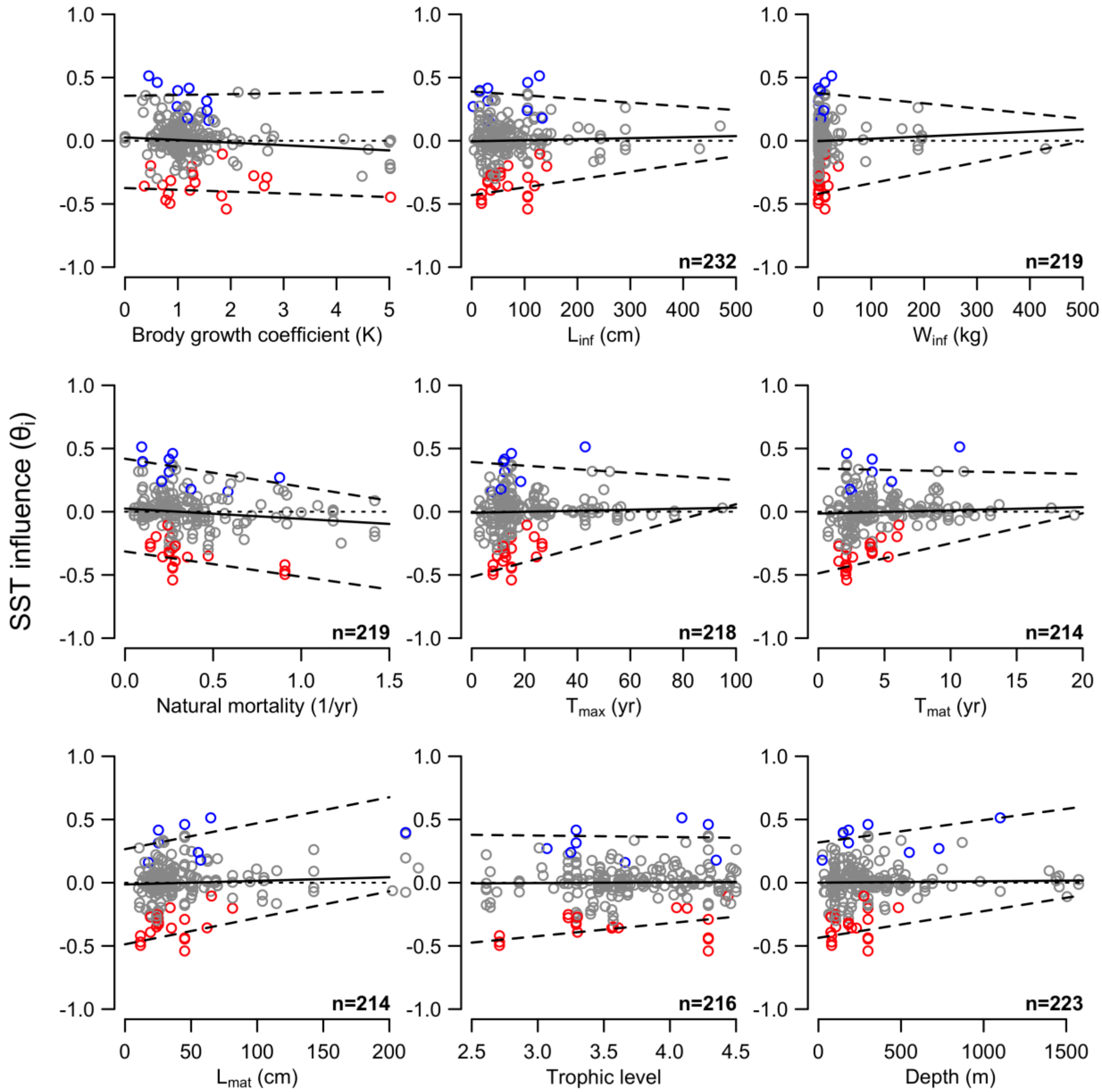

Fig. S19. **<u>SST influence as a function of nine life history traits.</u>** Life history traits are the: Brody growth coefficient (K), asymptotic maximum length (L_{inf}), asymptotic maximum weight (W_{inf}), natural mortality (M), maximum age (T_{max}), age at maturity (T_{mat}), length at maturity (L_{mat}), trophic level, and median depth. SST influences are colored by significance (blue=positive, red=negative, grey=non-significant). Solid lines show the 50th percentile quantile regression fit and dashed lines show the 2.5% and 97.5% quantile regression fits. Sample size is shown in the bottom-right corner if data were not available for all 235 stocks.

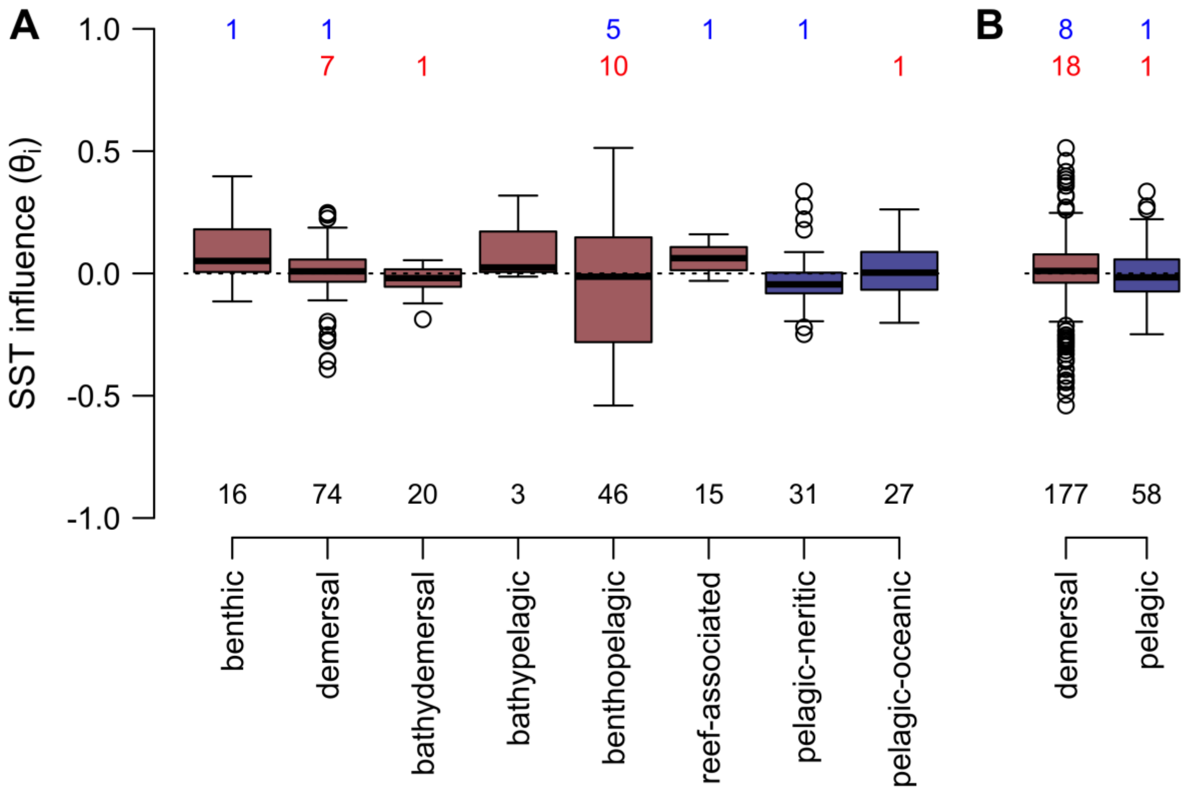

Fig. S20. **Distribution of SST influences among (A) specific and (B) generic habitat types.** Brown and blue boxplot shading corresponds to demersal and pelagic habitats, respectively. Black numbers indicate total number of stocks for each habitat type. Blue and red numbers show the number of stocks with a positive and negative SST influence, respectively.

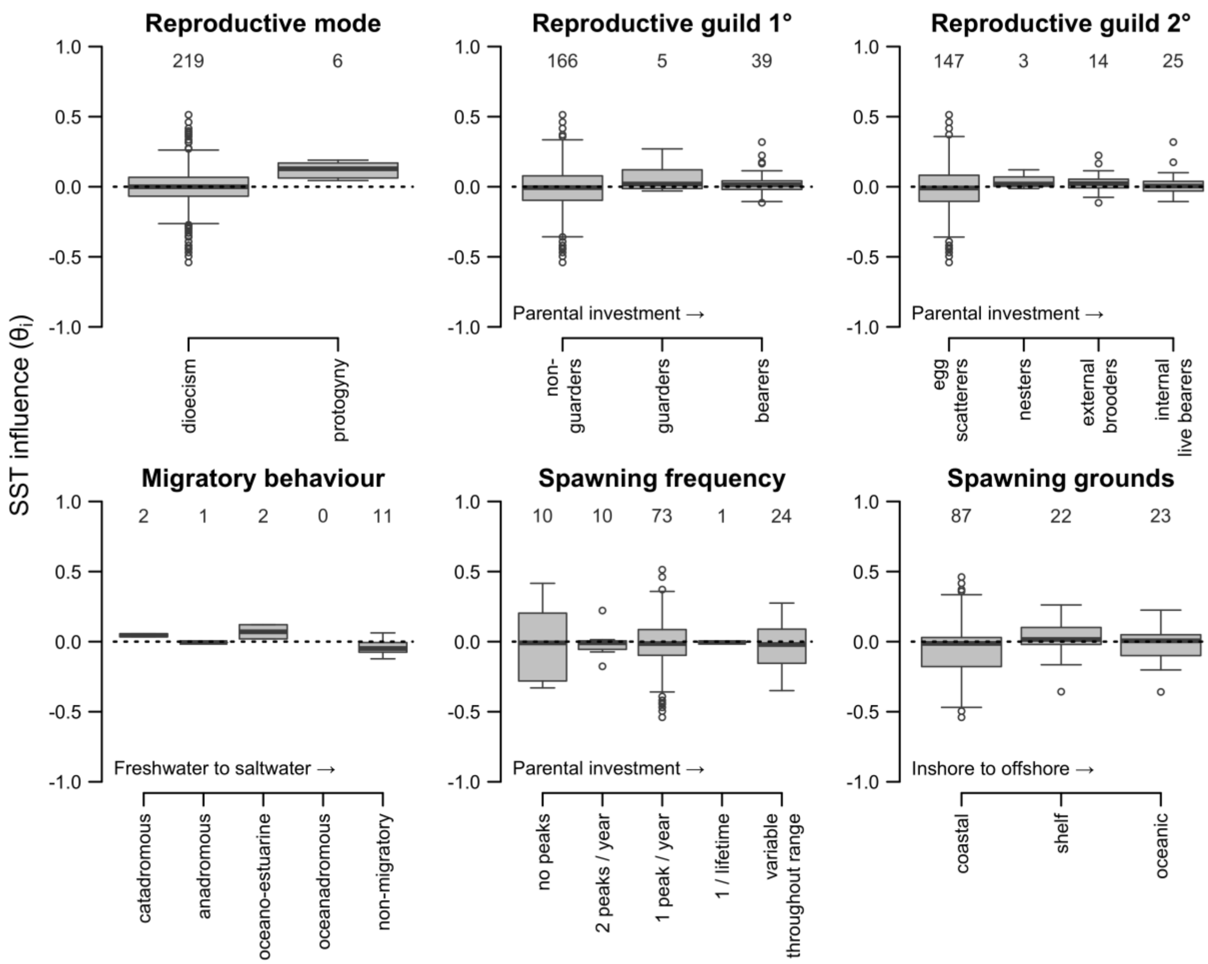

Fig. S21. **<u>Distribution of SST influences among reproductive strategies and migratory and spawning behaviors.</u>** Grey numbers indicate total number of stocks in each group.

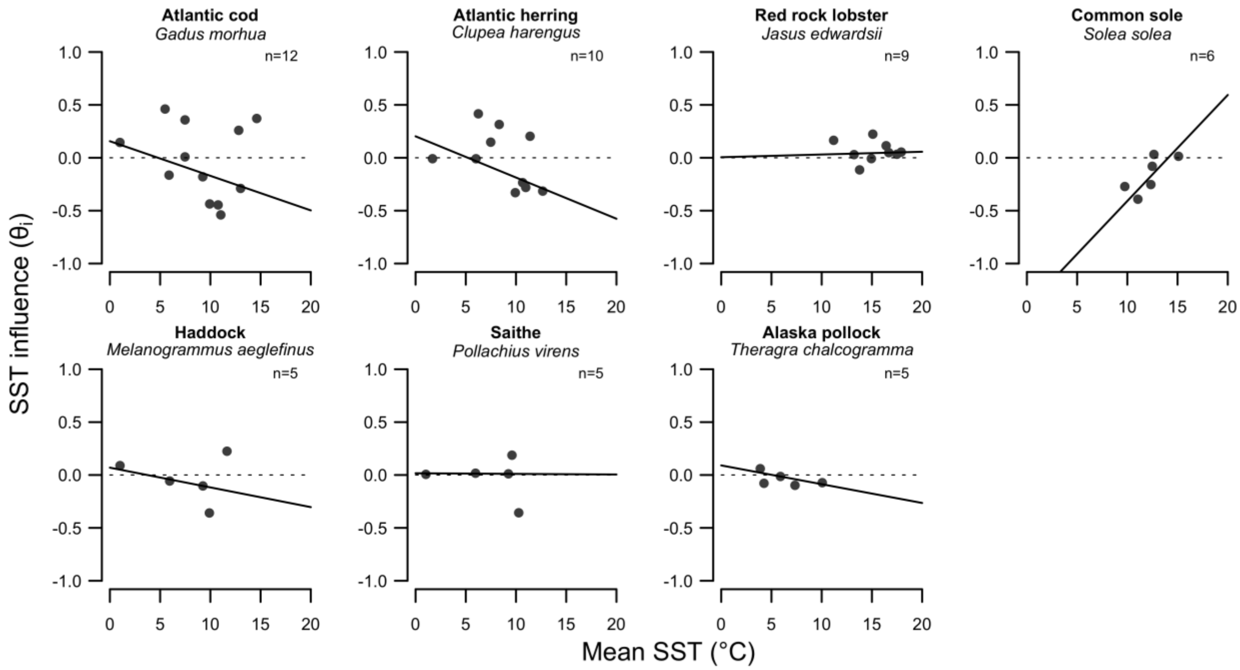

Fig. S22. SST influence as a function of the mean temperature experienced by stocks of the same species for the seven species with ≥5 stocks in the analysis. Lines show Theil-Sen regression fits. Theil-Sen regression, a form of robust regression, identifies the median slope of lines through all possible point pairs and is insensitive to outliers and endpoints in small datasets.

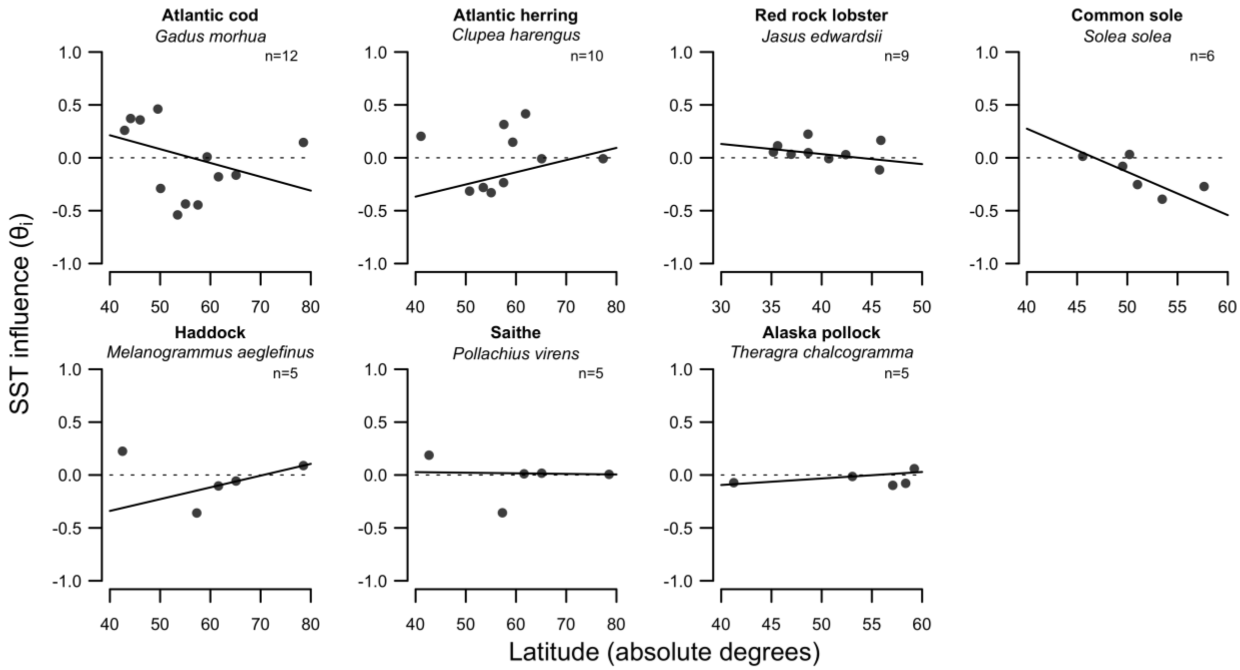

Fig. S23. <u>SST influence as a function of the latitude of stocks of the same species for the seven species with ≥5 stocks in the analysis.</u> Lines show Theil-Sen regression fits. Theil-Sen regression, a form of robust regression, identifies the median slope of lines through all possible point pairs and is insensitive to outliers and endpoints in small datasets.

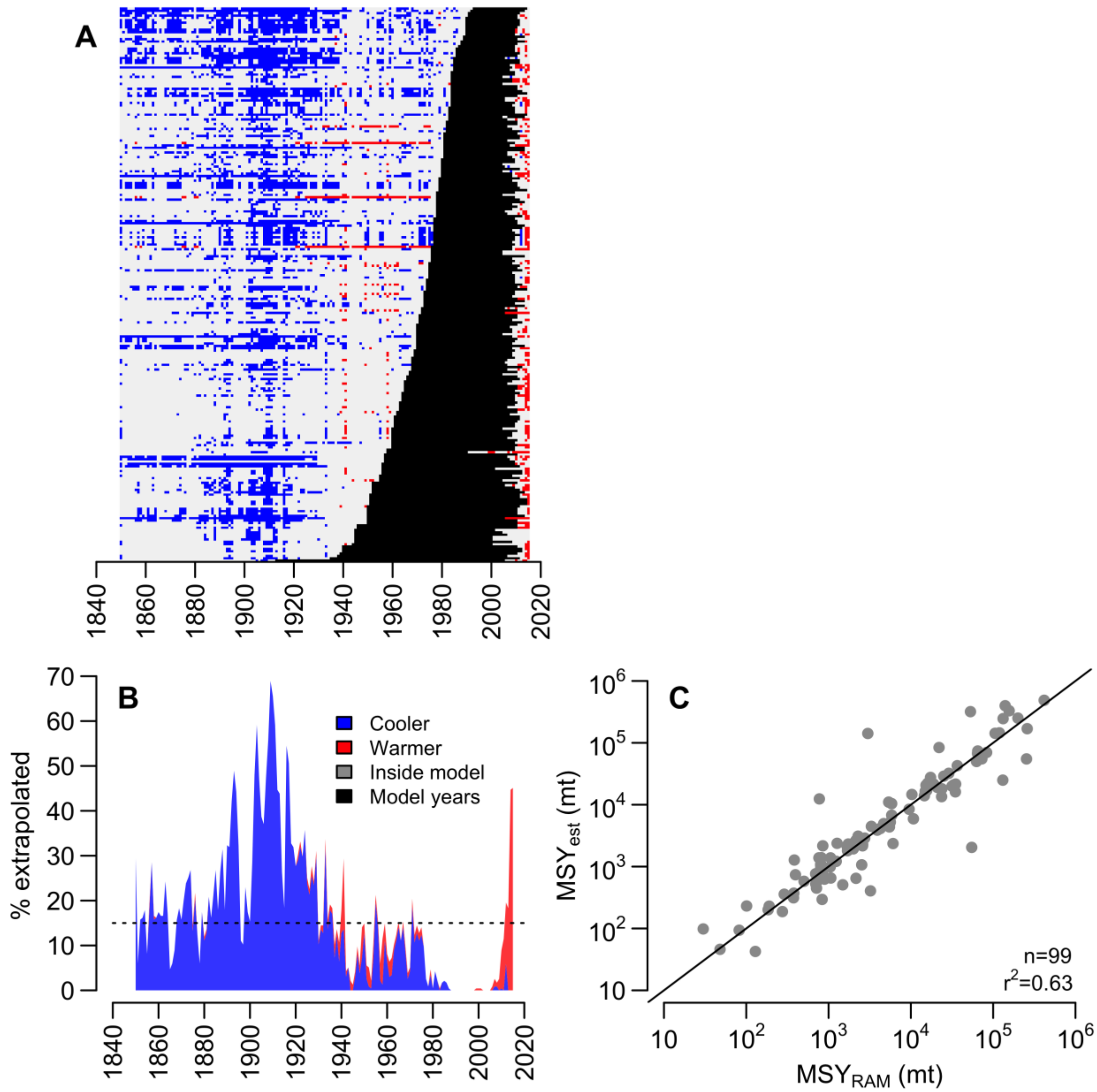

Fig. S24. **The (A&B) frequency of SST extrapolation by the hindcast model and (C) correlation between MSY estimates from the final model and data-rich stock assessments.** In (A), each row shows the SST experience of an individual stock where black years were used in model development, grey years experienced temperatures also experienced during model years, and blue and red years experienced temperatures cooler and warmer than those experienced during model years, respectively. In (B), the blue and red shading show the percentage of years experiencing temperatures cooler and warmer than those experienced during model years, respectively. The hindcast model generally extrapolates for fewer than 15% (dashed line) of years between 1930-2010. In (C), the diagonal line is the one-to-one line.

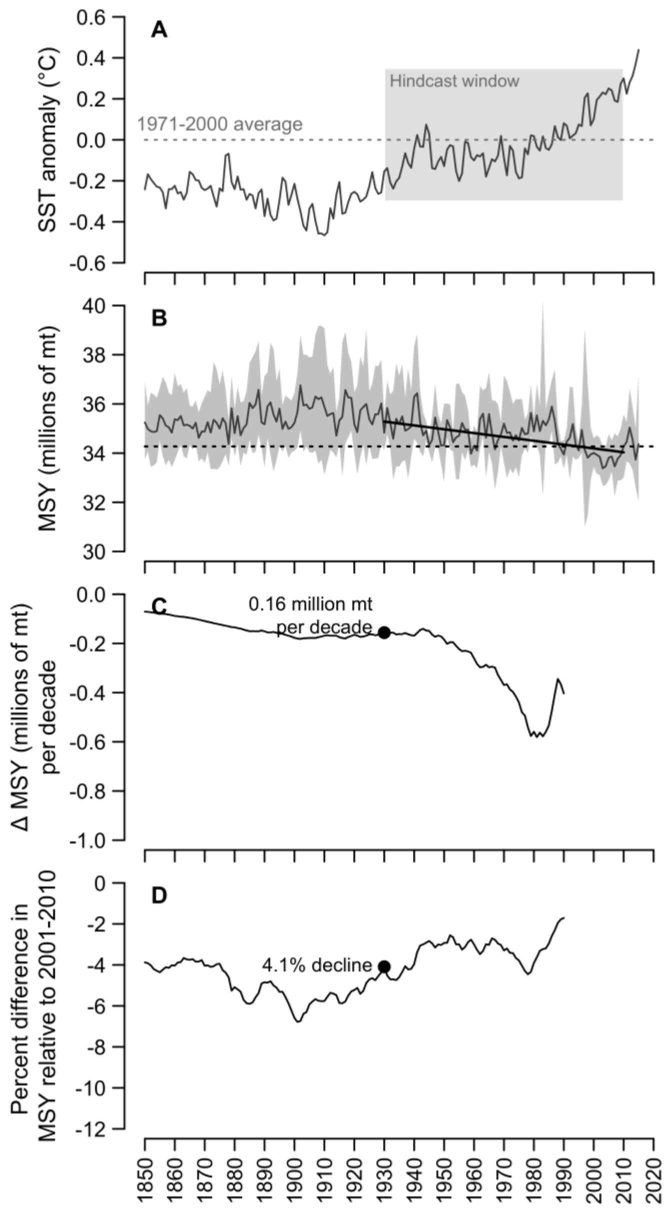

Fig. S25. **Sensitivity of hindcasted changes in MSY (mt=metric tons) to the determination of the hindcast window.** Time series showing (A) mean global SST anomaly, (B) hindcast of SST-dependent maximum sustainable yield (MSY) for all stocks included in the analysis, (C) Thiel-Sen regression slope when evaluating MSY trends beginning in each year from 1850-1990 and ending in 2010, and (D) percent difference in MSY when comparing the mean MSY over the 10 years following each year from 1850-1990 and the mean MSY from 2001-2010. In (A), the grey shading indicates the hindcast window determined to minimize extrapolation to temperatures outside those included in the final model. In (B), the dark line shows a Thiel-Sen regression fit to the MSY time series in the hindcast window. In (C) and (D), the labeled points mark the measures of MSY change experienced over the hindcast window.

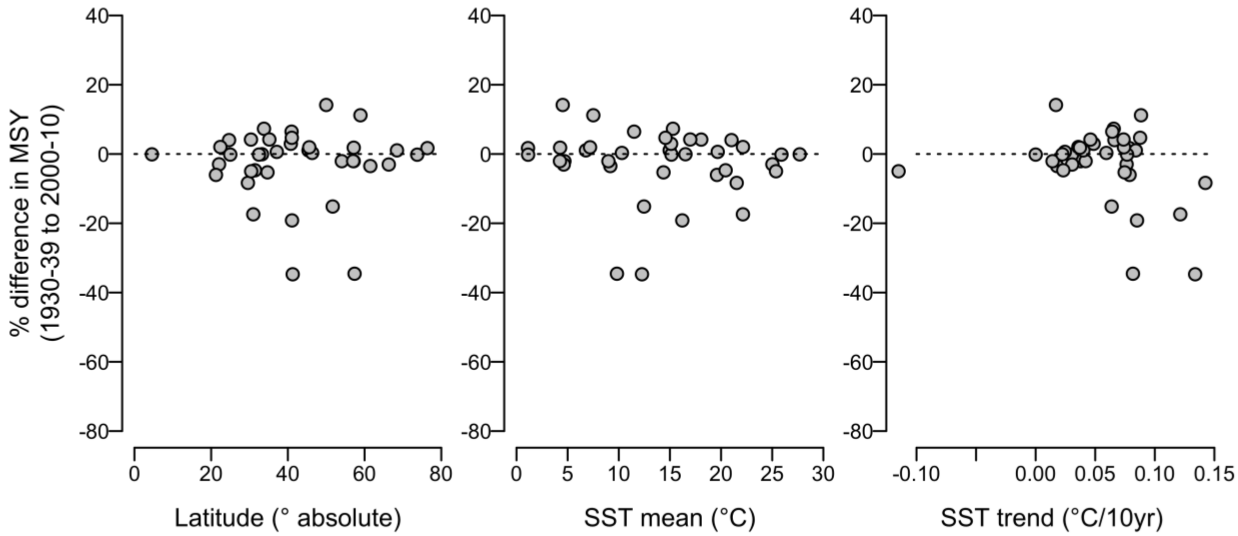

Fig. S26. <u>**Ecoregion-scale trends in maximum sustainable yield (MSY) related to ecoregion (A) latitude, (B) mean temperature, and (C) temperature trend.**</u>

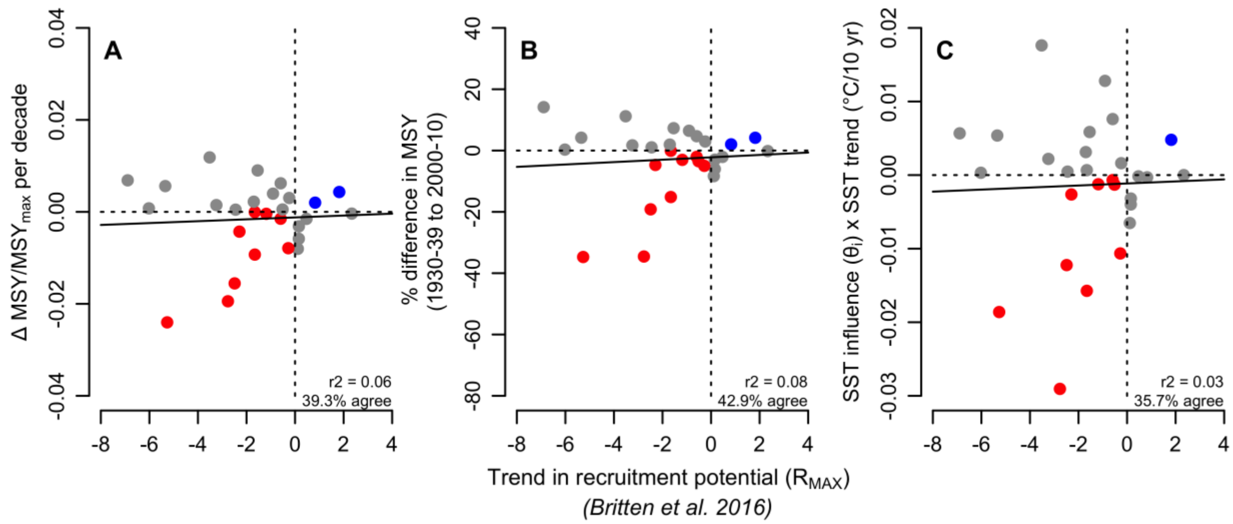

Fig. S27. **<u>Comparison of ecoregion-scale changes in fisheries productivity estimated by Britten et al. (*14*) and the present study.</u>** Britten et al. (*14*) quantify the meta-analytic mean trend in recruitment potential (R_{MAX}). Comparable values derived from the present study are: (A) change in scaled MSY (MSY divided by maximum MSY) per decade from 1930-2010; (B) percent difference in mean MSY from 1930-39 to 2001-2010; and (C) the meta-analytic mean of the SST influences of stocks in an ecoregion multiplied by the change in temperature from 1930-2010 in the ecoregion. In both studies, negative and positive values represent a negative and positive change, respectively. Blue and red points indicate ecoregions where both studies agree that change has positively and negatively impacted productivity, respectively. Grey points indicate ecoregions in which the studies disagree on the direction of productivity change. The present study describes SST influence for ten ecoregions not described in the Britten study (Bay of Biscay, Canary Current, Greenland Sea, Humboldt Current, Kuroshio Current, Labrador Sea, Mediterranean Sea, North Brazil Shelf, South Atlantic Ocean, and West Bering Sea) and the Britten study describes SST influence on one ecoregion not described in the present study (East-Central Australian Shelf).

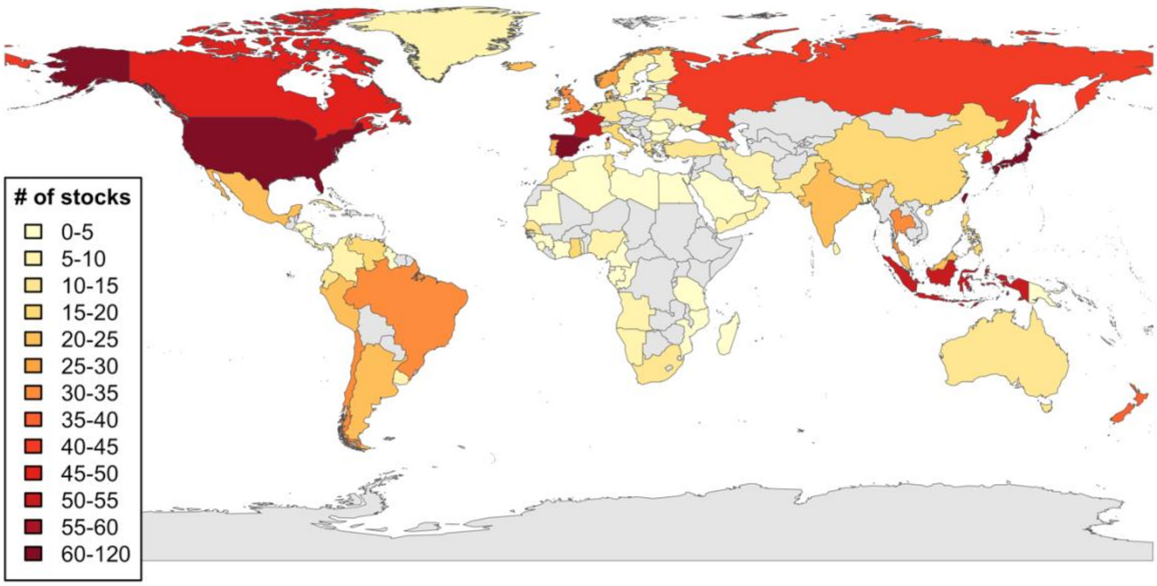

Fig. S28. **<u>Distribution of FAO stocks included in the vulnerability analysis</u>**. Each stock is a FAO area-country-species triple.

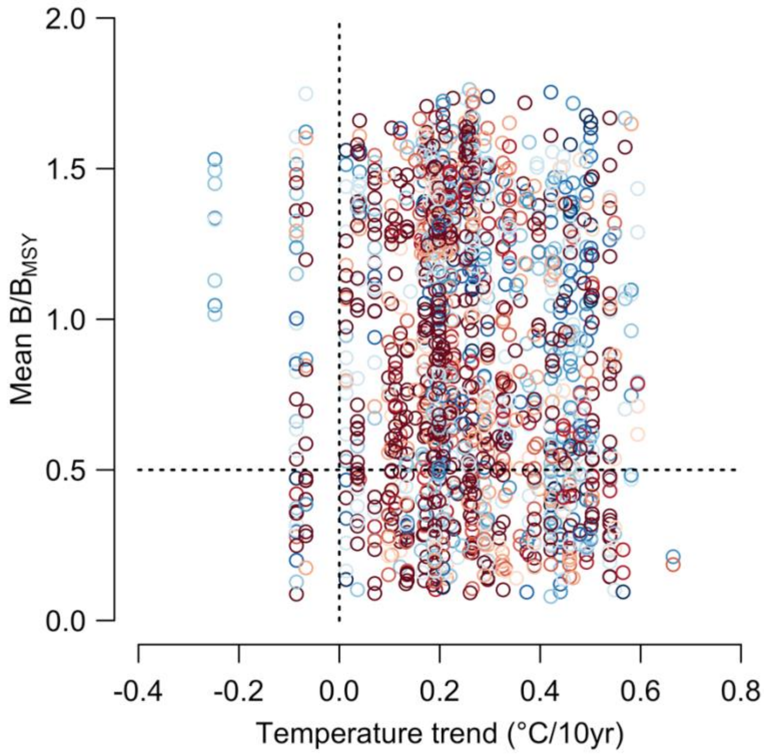

Fig. S29. <u>Indicators of the vulnerability of populations to ocean warming.</u> Points represent individual populations and are colored by the position of the population within its species-specific thermal niche (deep blue=coolest end of range; deep red=warmest end of range). Deep red populations in the bottom-right quadrant have experienced warming (positive temperature trend), overfishing (B/B_{MSY} < 0.5), and are located in the warm end of their thermal niche and are the most likely to be vulnerable to ocean warming.

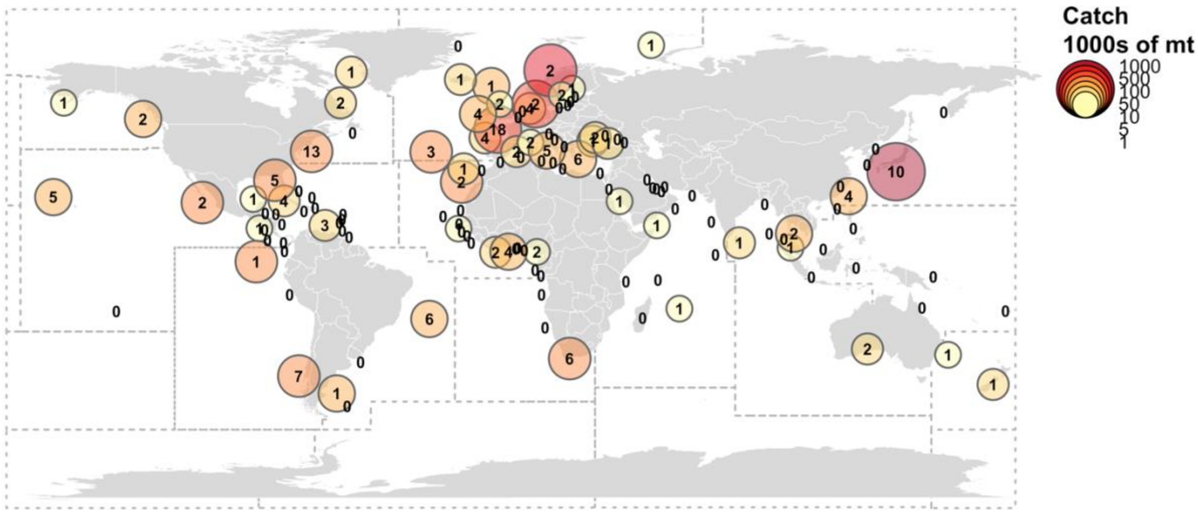

Fig. S30. <u>Number and total catch of populations vulnerable to warming by country (FAO region-country exclusive economic zone intersect).</u> Points are scaled and colored based on the total catch of vulnerable populations in each country and the number of vulnerable populations in each country is shown inside the point. Zeros indicate countries without any vulnerable populations. Dashed lines indicate FAO major fishing areas.

Supplemental Tables

Table S1. AIC of candidate surplus production models (PT=Pella-Tomlinson).

Model	K	Likelihood	AIC	ΔAIC
Question 1. Does asymmetry matter?				
PT model (MSY@45%K) **(standard model)**	940	-19280.4	-36680.9	0.0
Schaefer model (MSY@50%K)	940	-19278.9	-36677.8	3.1
PT model (MSY@40%K)	940	-19271.3	-36662.6	18.3
PT model (MSY@37%K)	940	-19261.1	-36642.1	38.8
Question 2. Does temperature matter?				
COBE SST-linked PT model **(base model)**	942	-19300.4	-36716.9	0.0
HadISST SST-linked PT model	942	-19290.5	-36697.0	19.9
ERSST SST-linked PT model	942	-19289.2	-36694.5	22.4
PT model (MSY@45%K) **(standard model)**	940	-19280.4	-36680.9	36.0
Question 3. Does group hierarchy matter?				
SST-linked PT model w/ hierarchy by ecoregion **(final model)**	943	-19312.0	-36738.0	0.0
SST-linked PT model w/ hierarchy by FAO area	943	-19309.3	-36732.7	5.3
SST-linked PT model w/ hierarchy by assessment method (specific)	943	-19306.4	-36726.7	11.3
SST-linked PT model w/ hierarchy by family	943	-19305.3	-36724.7	13.3
SST-linked PT model **(base model)**	942	-19300.4	-36716.9	21.1
SST-linked PT model w/ hierarchy by order	943	-19300.6	-36715.2	22.8
SST-linked PT model w/ hierarchy by assessment method (generic)	943	-19300.4	-36714.9	23.1
Question 4. Null model tests				
SST-linked PT model w/ hierarchy by LME **(final model)**	943	-19312.0	-36738.0	0.0
SST-linked PT model w/ hierarchy by LME - Null SST #2	943	-19285.1	-36684.1	53.8
SST-linked PT model w/ hierarchy by LME - Null SST #1	943	-19283.7	-36681.3	56.7
SST-linked PT model w/ hierarchy by LME - Null SST #3	943	-19280.5	-36674.9	63.0

Table S2. Stocks whose productivity is significantly influenced by ocean warming (sorted from most positive to most negative temperature influence).

Stock id	Species	Area	θ_i
GHAL4RST	Greenland halibut (*Reinhardtius hippoglossoides*)	Gulf of St. Lawrence	0.51
COD3Pn4RS	Atlantic cod (*Gadus morhua*)	Northern Gulf of St. Lawrence	0.46
HERR30	Atlantic herring (*Clupea harengus*)	Bothnian Sea	0.42
SCALLGB	Sea scallop (*Placopecten magellanicus*)	Georges Bank	0.40
HERRRIGA	Atlantic herring (*Clupea harengus*)	Gulf of Riga East of Gotland	0.31
PANDALGOM	Northern shrimp (*Pandalus borealis*)	Gulf of Maine	0.27
WHAKEGBGOM	White hake (*Urophycis tenuis*)	Gulf of Maine / Georges Bank	0.24
SPANMACKSATLC	Spanish mackerel (*Scomberomorus maculatus*)	Southern Atlantic coast	0.18
BSBASSMATLC	Black sea bass (*Centropristis striata*)	Mid-Atlantic Coast	0.16
KINGKLIPSA	Kingklip (*Genypterus capensis*)	South Africa	-0.11
ALBANATL	Albacore tuna (*Thunnus alalunga*)	Northern Atlantic	-0.20
ARFLOUNDBSAI	Arrowtooth flounder (*Atheresthes stomias*)	Bering Sea and Aleutian Islands	-0.20
PLAIC7d	European Plaice (*Pleuronectes platessa*)	Eastern English Channel	-0.25
SOLEIIIa	Common sole (*Solea solea*)	Kattegat and Skagerrak	-0.27
PLAICECHW	European Plaice (*Pleuronectes platessa*)	Western English Channel	-0.28
CODVIIek	Atlantic cod (*Gadus morhua*)	Celtic Sea	-0.29
HERRSIRS	Atlantic herring (*Clupea harengus*)	ICES VIIa-g-h-j	-0.32
HERRNS	Atlantic herring (*Clupea harengus*)	North Sea	-0.33
WHITNS-VIId	Whiting (*Merlangius merlangus*)	IV and VIId	-0.35
HADNS-IIIa	Haddock (*Melanogrammus aeglefinus*)	IIIa and North Sea	-0.36
POLLNS-VI-IIIa	Saithe (*Pollachius virens*)	IIIa, VI and North Sea	-0.36
SOLEIS	Common sole (*Solea solea*)	Irish Sea	-0.39
SEELNSSA1	Sand eel (*Ammodytes marinus*)	North Sea	-0.42
CODNS	Atlantic cod (*Gadus morhua*)	North Sea	-0.44
CODVIa	Atlantic cod (*Gadus morhua*)	West of Scotland	-0.45
SEELNSSA2	Sand eel (*Ammodytes marinus*)	North Sea	-0.47
SEELNSSA3	Sand eel (*Ammodytes marinus*)	North Sea	-0.50
CODIS	Atlantic cod (*Gadus morhua*)	Irish Sea	-0.54

Table S3. Potential predictors of temperature influence and their sources (percentage of stocks with predictor available shown in parenthesis when coverage is incomplete).

Variable	Source
SST experience	
SST average (°C)	COBE SST + stock boundary database (1930-2010)
SST trend (°C/yr)	COBE SST + stock boundary database (1930-2010)
Latitude (absolute value)	Centroid of the stock area (stock boundary database)
Stock characteristics	
Biomass average (MT)	RAM Legacy Database
Scaled biomass trend (scaled MT/yr)	RAM Legacy Database
Stock area (sq. km)	Stock boundary database
Time series length (year)	RAM Legacy Database
B/B_{MSY} average	RAM Legacy Database (52%)
F/F_{MSY} average	RAM Legacy Database (57%)
Geography	
Marine ecoregion	Containing the centroid of the stock area
FAO Major Fishing Area	Containing the centroid of the stock area
Life history traits	
Taxonomy (family/order)	RAM Legacy Database (corrected for errors)
Natural mortality rate (M, 1/yr)	FishLife (finfish, 100%), SeaLifeBase (inverts, 19%)
Brody growth coefficient (K)	FishLife (finfish, 100%), SeaLifeBase (inverts, 100%)
Asymptotic maximum length (L_{inf}, cm)	FishLife (finfish, 100%), SeaLifeBase (inverts, 38%)
Asymptotic maximum mass (W_{inf}, kg)	FishLife (finfish, 100%), SeaLifeBase (inverts, 24%)
Length at maturity (L_{mat}, cm)	FishLife (finfish, 100%), SeaLifeBase (inverts, 0%)
Age at maturity (T_{mat}, yr)	FishLife (finfish, 100%), SeaLifeBase (inverts, 0%)
Maximum age (T_{max}, yr)	FishLife (finfish, 100%), SeaLifeBase (inverts, 19%)
Trophic level	FishBase (finfish, 93%), SeaLifeBase (inverts, 19%)
Habitat (e.g., demersal, pelagic, etc.)	FishBase (finfish, 99%), SeaLifeBase (inverts, 95%)
Depth (m)	FishBase (finfish, 95%), SeaLifeBase (inverts, 0%)
Behavioral traits	
Migratory behavior (e.g., catadromous, etc.)	Fishbase (finfish, 69%), SeaLifeBase (inverts, 0%)
Reproductive mode (i.e., dioecism or protogyny)	Fishbase (finfish, 96%), SeaLifeBase (inverts, 95%)
Reproductive guild 1 (e.g., bearers, guarders, etc.)	Fishbase (finfish, 91%), SeaLifeBase (inverts, 71%)
Reproductive guild 2 (e.g., nesters, brooders, etc.)	Fishbase (finfish, 82%), SeaLifeBase (inverts, 67%)
Spawning ground (e.g., coastal, shelf, etc.)	Fishbase (finfish, 62%), SeaLifeBase (inverts, 0%)
Spawning frequency	Fishbase (finfish, 55%), SeaLifeBase (inverts, 5%)

Table S4. Hindcasted changes in SST-dependent maximum sustainable yield (MSY) from 1930-2010 among ecoregions (LME=large marine ecosystem; HSA=high seas area; sorted by ascending percent difference).

Type	Ecoregion	# of stocks	Total MSY (1000s of mt)	Mean SST (°C)	SST trend (°C / decade)	SST influence (θ_i)	MSY change mt / decade	MSY change % difference
LME	Sea of Japan	1	30.9	12.3	0.134	-0.14	-1119.7	-34.7
LME	North Sea	9	2454.6	9.8	0.082	-0.36	-78384.5	-34.6
LME	Iberian Coastal	2	3.1	16.2	0.085	-0.14	-59.8	-19.2
LME	Kuroshio Current	6	3720.8	22.1	0.121	-0.15	-67403.0	-17.4
LME	Celtic-Biscay Shelf	15	294.0	12.5	0.064	-0.25	-3278.4	-15.2
LME	East China Sea	5	1907.5	21.5	0.142	-0.05	-17185.3	-8.3
LME	Benguela Current	3	176.6	19.6	0.079	-0.05	-1120.1	-6.0
HSA	South Atlantic Ocean	1	25.2	14.4	0.075	-0.07	-180.2	-5.3
LME	Southeast U.S. Continental Shelf	9	20.4	25.4	-0.115	0.09	-176.0	-5.0
HSA	North Atlantic Ocean	6	328.8	20.4	0.023	-0.11	-1440.5	-4.7
LME	Faroe Plateau	3	86.7	9.2	0.018	-0.07	48.2	-3.5
LME	Iceland Shelf and Sea	5	1261.0	4.6	0.031	-0.04	-554.0	-3.0
LME	Agulhas Current	5	761.2	25.0	0.076	-0.04	-2503.2	-3.0
LME	Gulf of Alaska	20	356.2	9.0	0.014	-0.01	-586.8	-2.1
LME	East Bering Sea	14	3297.4	4.7	0.038	-0.02	-5306.8	-2.1
HSA	Labrador Sea	2	138.5	4.2	0.042	-0.05	66.7	-2.0
LME	Greenland Sea	1	1029.3	1.1	0.031	-0.01	-108.1	-0.2
LME	Gulf of Mexico	3	2.0	25.9	0.000	0.01	-0.7	-0.2
LME	Humboldt Current	16	10178.6	15.1	0.077	-0.01	28.6	-0.2
LME	North Brazil Shelf	1	17.3	27.7	0.022	0.00	-1.1	-0.1
LME	California Current	29	286.5	16.5	0.034	0.02	-14.5	-0.1
LME	Patagonian Shelf	2	349.2	10.3	0.059	0.01	270.7	0.3
LME	Mediterranean Sea	2	40.1	19.7	0.025	0.01	11.3	0.6
HSA	Bay of Biscay	1	7.2	15.0	0.084	0.01	6.2	1.0
LME	Norwegian Sea	1	1262.7	6.8	0.040	0.01	614.4	1.1

LME	Barents Sea	5	2633.8	1.1	0.079	0.03	3967.5	1.7
LME	West Bering Sea	1	143.3	4.3	0.037	0.03	35.7	1.8
LME	Scotian Shelf	2	41.0	7.2	0.074	0.04	94.0	1.9
HSA	North Pacific Ocean	4	149.6	22.1	0.036	-0.01	304.4	2.0
LME	New Zealand Shelf	9	5.8	15.1	0.049	0.03	18.5	3.0
LME	Canary Current	2	712.9	21.0	0.066	0.04	2228.8	4.0
HSA	South Pacific Ocean	5	86.7	18.1	0.046	0.10	387.7	4.2
LME	South West Australian Shelf	5	2.8	17.0	0.074	0.07	16.2	4.2
LME	Southeast Australian Shelf	8	9.2	14.6	0.088	0.09	60.2	4.7
LME	Northeast U.S. Continental Shelf	15	878.0	11.5	0.064	0.20	4096.5	6.5
HSA	Indian Ocean	4	452.4	15.3	0.066	0.09	4374.6	7.3
LME	Baltic Sea	5	828.7	7.5	0.088	0.20	11597.4	11.2
LME	Labrador - Newfoundland	8	292.0	4.5	0.017	0.33	2802.3	14.2

Table S5. RAM Legacy Database stocks used in analysis (TB = total biomass).

Condition	# of stocks
All RAMLDB stocks	1058
Not Pacific salmon stocks	685
Only stocks with TB/catch in metric tons	350
Only stocks with TB/catch time series ≥ 20 years	300
Removed 23 stocks with strong SP/SR relationships	277
Removed 9 stocks without 20 years of data after trimming	268
Removed 5 stocks without SST data (e.g., Seto Sea not covered by COBE)	263
Removed 28 stocks preventing model convergence	235

Table S6. Model symbols and their definitions.

Type	Symbol	Definition
Data	$C_{i,t}$	Catch for stock *i* in year *t*
Data	$SP_{i,t}$	Surplus production for stock *i* in year *t*
Data	$B_{i,t}$	Total biomass for stock *i* in year *t*
Data	$SST_{i,t}$	Sea surface temperature (SST) experienced by stock *i* in year *t*
Data	G_i	Group (taxonomic, geographic, or stock assessment model) for stock *i*
Derived	$\varepsilon_{i,t}$	Residual process variability for stock *i* in year *t*
Parameter	r_i	Intrinsic rate of growth for stock *i*
Parameter	K_i	Carrying capacity for stock *i*
Parameter	θ_i	Influence of SST on productivity for stock *i*
Parameter	μ_{SST}	Mean of the distribution of SST influences (θ_i)
Parameter	σ_{SST}	Standard deviation of the distribution of SST influences (θ_i)
Parameter	$\mu_{G,j}$	Mean of the distribution of SST influences (θ_i) for group *j*
Parameter	σ_G	Standard deviation of the group-specific distributions of SST influences (θ_i)
Parameter	$\sigma_{P,i}$	Standard deviation of the residual process variability for stock *i*
Parameter	ρ_i	First-order (AR1) autocorrelation coefficient for stock *i*
Constant	p	Shape parameter: fixed at 1.00, 0.55, 0.20, or 0.01
Index	t	Year
Index	i	Stock
Index	j	Group (taxonomic or geographic)

Table S7. Stock assessment methods represented in the data.

Assessment model	Number	Countries
Biomass dynamics model (n=30)		
BSPM: Bayesian surplus production model	10	Canada, Tuna-RFMO
ASPIC: Surplus production model	6	Tuna-RFMO, USA
Delay difference model	5	Canada, USA
ASPM: Age-structured surplus production model	4	South Africa
DPM: Dynamic production model	2	West Africa
qR: Surplus production model	2	Australia
LPM: Logistic production model	1	Canada
Integrated analysis (n=57)		
SS3: Stock Synthesis v3.0 model	26	Australia, Europe, Tuna-RFMO, USA
SS2: Stock Synthesis v2.0 model	22	Australia, USA
SMS: Stochastic multi-species model	3	Europe
CASAL: C++ Algorithmic Stock Assessment Laboratory	2	New Zealand
IA: Integrated analysis	1	USA
JJM: Joint jack mackerel	1	Chile
SS1: Stock Synthesis v1.0 model	1	USA
SYM: Stochastic yield model	1	USA
Statistical catch-at-age model (n=55)		
AD-CAM: AD-Model Builder statistical catch-at-age model	20	Europe, South Africa, USA
SCA: Statistical catch-at-age model	8	Canada, Europe, Tuna-RFMO, USA
ASAP: Age Structured Assessment Program	6	USA
BAM: Beaufort assessment model	6	USA
ICA: Integrated catch-at-age analysis	5	Europe
TSA: State-space catch-at-age time series analysis	4	Canada, Europe
MULTIFAN-CL: Length-based, age/spatially-structured model	2	Tuna-RFMO
SAM: State-space assessment model	2	Europe

CSA: Catch-survey analysis (like a state space approach)	1	USA
SCALE: A statistical catch-at-length model	1	USA
Statistical catch-at-length model (n=3)		
AD-CAL: AD-Model Builder catch-at-length model	2	USA
LBA: Length-based analysis	1	USA
Survey index (n=5)		
Temporal indices derived from scientific survey data	3	USA
SURBA: Survey-based stock assessment method	2	Canada
Unknown (n=38)		
Unknown	27	Canada, Chile, Europe, Peru, South Africa, USA
MSLM: Multi-stock length-based model	7	New Zealand
SnapEst: SnapEst age- and length-based model	2	Australia
CapTool: Spreadsheet assessment model used for capelin	1	Europe
RYM: Replacement yield model	1	South Africa
Virtual population analysis (n=47)		
XSA: Extended survivor analysis	26	Argentina, Canada, Europe, Tuna-RFMO
VPA: Virtual population analysis	16	Argentina, Canada, Europe, Japan, Russia
ADAPT: Adaptive framework-virtual population analysis	1	Europe
B-ADAPT: ADAPT approach with year effects in a catch multiplier	1	Europe
FLXSA: FLR variant of extended survivor analysis	1	Europe
NFT-ADAPT: VPA/ADPAT version 2.3.2 NOAA Fisheries	1	Europe
SPA-ADAPT: Sequential population analysis / ADAPT	1	Canada

Table S8. AFS and FishBase guidelines for using life history traits to classify the resilience of fish stocks to exploitation and the r priors used by catch-MSY for each resilience category.*

Resilience	r prior	Von B K (1/yr)	Maximum age (yr)	Age at maturity (yr)
High	[0.6, 1.5]	>0.3	1-3	<1
Medium	[0.2, 1.0]	0.16-0.30	4-10	2-4
Low	[0.05, 0.5]	0.05-0.15	11-30	5-10
Very low	[0.015, 0.1]	<0.05	> 30	>10
Unknown	[0.2, 1.0]	------	------	------

* Resilience categories were assigned using, in order of preference, resilience values: (1) reported on FB/SLB; (2) derived from the FishLife Von Bertalanffy growth parameter; (3) derived from the FB/SLB Von Bertalanffy growth parameter; (4) derived from the FB/SLB vulnerability metric; (5) derived from the FB/SLB Von Bertalanffy maximum age; (6) derived from the genus mode; or (7) derived from the family mode.

References and Notes

1. Food and Agriculture Organization (FAO), "The state of world fisheries and aquaculture 2016" (Food and Agriculture Organization of the United Nations, 2016).

2. H. C. J. Godfray, J. R. Beddington, I. R. Crute, L. Haddad, D. Lawrence, J. F. Muir, J. Pretty, S. Robinson, S. M. Thomas, C. Toulmin, Food security: The challenge of feeding 9 billion people. *Science* **327**, 812–818 (2010). doi:10.1126/science.1185383 Medline

3. S. Manabe, R. J. Stouffer, Century-scale effects of increased atmospheric CO_2 on the ocean–atmosphere system. *Nature* **364**, 215–218 (1993). doi:10.1038/364215a0

4. R. E. Keeling, A. Körtzinger, N. Gruber, Ocean deoxygenation in a warming world. *Ann. Rev. Mar. Sci.* **2**, 199–229 (2010). doi:10.1146/annurev.marine.010908.163855 Medline

5. L. Bopp, L. Resplandy, J. C. Orr, S. C. Doney, J. P. Dunne, M. Gehlen, P. Halloran, C. Heinze, T. Ilyina, R. Séférian, J. Tjiputra, M. Vichi, Multiple stressors of ocean ecosystems in the 21st century: Projections with CMIP5 models. *Biogeosciences* **10**, 6225–6245 (2013). doi:10.5194/bg-10-6225-2013

6. M. L. Pinsky, B. Worm, M. J. Fogarty, J. L. Sarmiento, S. A. Levin, Marine taxa track local climate velocities. *Science* **341**, 1239–1242 (2013). doi:10.1126/science.1239352 Medline

7. C. Deutsch, A. Ferrel, B. Seibel, H. O. Pörtner, R. B. Huey, Climate change tightens a metabolic constraint on marine habitats. *Science* **348**, 1132–1135 (2015). doi:10.1126/science.aaa1605 Medline

8. C. A. Stock, J. G. John, R. R. Rykaczewski, R. G. Asch, W. W. L. Cheung, J. P. Dunne, K. D. Friedland, V. W. Y. Lam, J. L. Sarmiento, R. A. Watson, Reconciling fisheries catch and ocean productivity. *Proc. Natl. Acad. Sci. U.S.A.* **114**, E1441–E1449 (2017). doi:10.1073/pnas.1610238114 Medline

9. W. W. L. Cheung, G. Reygondeau, T. L. Frölicher, Large benefits to marine fisheries of meeting the 1.5°C global warming target. *Science* **354**, 1591–1594 (2016). doi:10.1126/science.aag2331 Medline

10. J. L. Blanchard, S. Jennings, R. Holmes, J. Harle, G. Merino, J. I. Allen, J. Holt, N. K. Dulvy, M. Barange, Potential consequences of climate change for primary production and fish production in large marine ecosystems. *Philos. Trans. R. Soc. London Ser. B* **367**, 2979–2989 (2012). doi:10.1098/rstb.2012.0231 Medline

11. M. Barange, G. Merino, J. L. Blanchard, J. Scholtens, J. Harle, E. H. Allison, J. I. Allen, J. Holt, S. Jennings, Impacts of climate change on marine ecosystem production in societies dependent on fisheries. *Nat. Clim. Chang.* **4**, 211–216 (2014). doi:10.1038/nclimate2119

12. J. K. Moore, W. Fu, F. Primeau, G. L. Britten, K. Lindsay, M. Long, S. C. Doney, N. Mahowald, F. Hoffman, J. T. Randerson, Sustained climate warming drives declining marine biological productivity. *Science* **359**, 1139–1143 (2018). doi:10.1126/science.aao6379 Medline

13. Intergovernmental Panel on Climate Change (IPCC), "Climate change 2013: The physical science basis. Contribution to the fifth assessment report of the Intergovernmental Panel on Climate Change" (Cambridge Univ. Press, 2013).

14. G. L. Britten, M. Dowd, B. Worm, Changing recruitment capacity in global fish stocks. *Proc. Natl. Acad. Sci. U.S.A.* **113**, 134–139 (2016). doi:10.1073/pnas.1504709112 Medline

15. P. A. Larkin, An epitaph for the concept of maximum sustained yield. *Trans. Am. Fish. Soc.* **106**, 1–11 (1977). doi:10.1577/1548-8659(1977)106<1:AEFTCO>2.0.CO;2

16. K. D. Friedland, C. Stock, K. F. Drinkwater, J. S. Link, R. T. Leaf, B. V. Shank, J. M. Rose, C. H. Pilskaln, M. J. Fogarty, Pathways between primary production and fisheries yields of large marine ecosystems. *PLOS ONE* **7**, e28945 (2012). doi:10.1371/journal.pone.0028945 Medline

17. J. J. Pella, P. K. Tomlinson, A generalized stock production model. *Inter Am. Trop. Tuna Comm. Bull.* **13**, 421–454 (1969).

18. M. Ishii, A. Shouji, S. Sugimoto, T. Matsumoto, Objective analyses of sea-surface temperature and marine meteorological variables for the 20th century using ICOADS and the Kobe Collection. *Int. J. Climatol.* **25**, 865–879 (2005). doi:10.1002/joc.1169

19. D. Ricard, C. Minto, O. P. Jensen, J. K. Baum, Examining the knowledge base and status of commercially exploited marine species with the RAM Legacy Stock Assessment Database. *Fish Fish.* **13**, 380–398 (2012). doi:10.1111/j.1467-2979.2011.00435.x

20. Materials and methods are available as supplementary materials.

21. H. Akaike, A new look at the statistical model identification. *IEEE Trans. Automat. Contr.* **19**, 716–723 (1974). doi:10.1109/TAC.1974.1100705

22. F. J. Mueter, C. Broms, K. F. Drinkwater, K. D. Friedland, J. A. Hare, G. L. Hunt Jr., W. Melle, M. Taylor, Ecosystem responses to recent oceanographic variability in high-latitude Northern Hemisphere ecosystems. *Prog. Oceanogr.* **81**, 93–110 (2009). doi:10.1016/j.pocean.2009.04.018

23. A. J. Richardson, D. S. Schoeman, Climate impact on plankton ecosystems in the Northeast Atlantic. *Science* **305**, 1609–1612 (2004). doi:10.1126/science.1100958 Medline

24. L. W. Clausen, A. Rindorf, M. van Deurs, M. Dickey-Collas, N. T. Hintzen, Shifts in North Sea forage fish productivity and potential fisheries yield. *J. Appl. Ecol.* **51**, 45 (2017).

25. G. Beaugrand, K. M. Brander, J. Alistair Lindley, S. Souissi, P. C. Reid, Plankton effect on cod recruitment in the North Sea. *Nature* **426**, 661–664 (2003). doi:10.1038/nature02164 Medline

26. B. R. MacKenzie, F. W. Köster, Fish production and climate: Sprat in the Baltic Sea. *Ecology* **85**, 784–794 (2004). doi:10.1890/02-0780

27. V. Bartolino, P. Margonski, M. Lindegren, H. W. Linderholm, M. Cardinale, D. Rayner, H. Wennhage, M. Casini, Forecasting fish stock dynamics under climate change: Baltic herring (*Clupea harengus*) as a case study. *Fish. Oceanogr.* **23**, 258–269 (2014). doi:10.1111/fog.12060

28. A. D. Rijnsdorp, M. A. Peck, G. H. Engelhard, C. Möllmann, J. K. Pinnegar, Resolving the effect of climate change on fish populations. *ICES J. Mar. Sci.* **66**, 1570–1583 (2009). doi:10.1093/icesjms/fsp056

29. V. S. Saba, S. M. Griffies, W. G. Anderson, M. Winton, M. A. Alexander, T. L. Delworth, J. A. Hare, M. J. Harrison, A. Rosati, G. A. Vecchi, R. Zhang, Enhanced warming of the Northwest Atlantic Ocean under climate change. *J. Geophys. Res. Oceans* **121**, 118–132 (2016). doi:10.1002/2015JC011346

30. H. O. Pörtner, R. Knust, Climate change affects marine fishes through the oxygen limitation of thermal tolerance. *Science* **315**, 95–97 (2007). doi:10.1126/science.1135471 Medline

31. A. L. Perry, P. J. Low, J. R. Ellis, J. D. Reynolds, Climate change and distribution shifts in marine fishes. *Science* **308**, 1912–1915 (2005). doi:10.1126/science.1111322 Medline

32. S. D. Gaines, C. Costello, B. Owashi, T. Mangin, J. Bone, J. G. Molinos, M. Burden, H. Dennis, B. S. Halpern, C. V. Kappel, K. M. Kleisner, D. Ovando, Improved fisheries management could offset many negative effects of climate change. *Sci. Adv.* **4**, o1378 (2018). doi:10.1126/sciadv.aao1378 Medline

33. L. A. K. Barnett, T. A. Branch, R. A. Ranasinghe, T. E. Essington, Old-growth fishes become scarce under fishing. *Curr. Biol.* **27**, 2843–2848.e2 (2017). doi:10.1016/j.cub.2017.07.069 Medline

34. E. M. Olsen, M. Heino, G. R. Lilly, M. J. Morgan, J. Brattey, B. Ernande, U. Dieckmann, Maturation trends indicative of rapid evolution preceded the collapse of northern cod. *Nature* **428**, 932–935 (2004). doi:10.1038/nature02430 Medline

35. D. R. Barneche, D. R. Robertson, C. R. White, D. J. Marshall, Fish reproductive-energy output increases disproportionately with body size. *Science* **360**, 642–645 (2018). doi:10.1126/science.aao6868 Medline

36. B. Planque, J.-M. Fromentin, P. Cury, K. F. Drinkwater, S. Jennings, R. I. Perry, S. Kifani, How does fishing alter marine populations and ecosystems sensitivity to climate? *J. Mar. Syst.* **79**, 403–417 (2010). doi:10.1016/j.jmarsys.2008.12.018

37. C.-H. Hsieh, C. S. Reiss, J. R. Hunter, J. R. Beddington, R. M. May, G. Sugihara, Fishing elevates variability in the abundance of exploited species. *Nature* **443**, 859–862 (2006). doi:10.1038/nature05232 Medline

38. A. O. Shelton, M. Mangel, Fluctuations of fish populations and the magnifying effects of fishing. *Proc. Natl. Acad. Sci. U.S.A.* **108**, 7075–7080 (2011). doi:10.1073/pnas.1100334108 Medline

39. M. L. Pinsky, D. Byler, Fishing, fast growth and climate variability increase the risk of collapse. *Proc. R. Soc. London Ser. B* **282**, 20151053 (2015). doi:10.1098/rspb.2015.1053 Medline

40. G. L. Britten, M. Dowd, L. Kanary, B. Worm, Extended fisheries recovery timelines in a changing environment. *Nat. Commun.* **8**, 15325 (2017). doi:10.1038/ncomms15325 Medline

41. United Nations Department of Economic and Social Affairs (UN-DESA), "World population prospects: The 2017 revision, key findings and advance tables" (Working paper no. ESA/P/WP/248, UN-DESA, 2017).

42. W. W. L. Cheung, V. W. Lam, J. L. Sarmiento, K. Kearney, R. Watson, D. Zeller, D. Pauly, Large-scale redistribution of maximum fisheries catch potential in the global ocean under climate change. *Global Change Biol.* **16**, 24–35 (2010). doi:10.1111/j.1365-2486.2009.01995.x

43. H. K. Cha, S. Jung, Fishing vs. climate change: An example of filefish (*Thamnaconus modestus*) in the northern East China Sea. *J. Mar. Sci. Technol.* **21**, 15–22 (2013).

44. C. S. Szuwalski, M. G. Burgess, C. Costello, S. D. Gaines, High fishery catches through trophic cascades in China. *Proc. Natl. Acad. Sci. U.S.A.* **114**, 717–721 (2017). doi:10.1073/pnas.1612722114 Medline

45. K. M. Brander, Global fish production and climate change. *Proc. Natl. Acad. Sci. U.S.A.* **104**, 19709–19714 (2007). doi:10.1073/pnas.0702059104 Medline

46. E. N. Brooks, J. J. Deroba, When "data" are not data: The pitfalls of post hoc analyses that use stock assessment model output. *Can. J. Fish. Aquat. Sci.* **72**, 634–641 (2015). doi:10.1139/cjfas-2014-0231

47. J. T. Thorson, J. M. Cope, K. M. Kleisner, J. F. Samhouri, A. O. Shelton, E. J. Ward, Giants' shoulders 15 years later: Lessons, challenges and guidelines in fisheries meta-analysis. *Fish Fish.* **16**, 342–361 (2013). doi:10.1111/faf.12061

48. K. F. Drinkwater, G. Beaugrand, M. Kaeriyama, S. Kim, G. Ottersen, R. I. Perry, H.-O. Pörtner, J. J. Polovina, A. Takasuka, On the processes linking climate to ecosystem changes. *J. Mar. Syst.* **79**, 374–388 (2010). doi:10.1016/j.jmarsys.2008.12.014

49. A. E. Raftery, A. Zimmer, D. M. W. Frierson, R. Startz, P. Liu, Less than 2°C warming by 2100 unlikely. *Nat. Clim. Chang.* **7**, 637–641 (2017). doi:10.1038/nclimate3352 Medline

50. RAM Legacy Stock Assessment Data Base; www.ramlegacy.org.

51. COBE sea surface temperature dataset; www.esrl.noaa.gov/psd/data/gridded/data.cobe.html.

52. C. M. Free, sst_productivity, GitHub; https://github.com/cfree14/sst_productivity.

53. B. Huang, V. F. Banzon, E. Freeman, J. Lawrimore, W. Liu, T. C. Peterson, T. M. Smith, P. W. Thorne, S. D. Woodruff, H.-M. Zhang, Extended Reconstructed Sea Surface Temperature Version 4 (ERSST.v4). Part I: Upgrades and intercomparisons. *J. Clim.* **28**, 911–930 (2015). doi:10.1175/JCLI-D-14-00006.1

54. N. A. Rayner, Global analyses of sea surface temperature, sea ice, and night marine air temperature since the late nineteenth century. *J. Geophys. Res.* **108**, 4407 (2003). doi:10.1029/2002JD002670

55. M. B. Schaefer, Some aspects of the dynamics of populations important to the management of the commercial marine fisheries. *Inter Am. Trop. Tuna Comm. Bull.* **1**, 27–56 (1954).

56. W. W. Fox Jr., An exponential surplus-yield model for optimizing exploited fish populations. *Trans. Am. Fish. Soc.* **99**, 80–88 (1970). doi:10.1577/1548-8659(1970)99<80:AESMFO>2.0.CO;2

57. J. T. Thorson, J. M. Cope, T. A. Branch, O. P. Jensen, Spawning biomass reference points for exploited marine fishes, incorporating taxonomic and body size information. *Can. J. Fish. Aquat. Sci.* **69**, 1556–1568 (2012). doi:10.1139/f2012-077

58. K. Kristensen, A. Nielsen, C. W. Berg, H. Skaug, B. M. Bell, TMB: Automatic differentiation and Laplace approximation. *J. Stat. Softw.* **70**, 1–21 (2016). doi:10.18637/jss.v070.i05

59. R Core Team, R: A language and environment for statistical computing; www.R-project.org/.

60. NOAA, Large Marine Ecosystems of the World; http://lme.edc.uri.edu/index.php.

61. VLIZ, IHO Sea Areas, version 2; www.marineregions.org/.

62. R. J. Hyndman, forecast: Forecasting functions for time series and linear models (R package version 8.2, 2018).

63. S. Martell, R. Froese, A simple method for estimating MSY from catch and resilience. *Fish Fish.* **14**, 504–514 (2012). doi:10.1111/j.1467-2979.2012.00485.x

64. S. C. Anderson, A. B. Cooper, O. P. Jensen, C. Minto, J. T. Thorson, J. C. Walsh, J. Afflerbach, M. Dickey-Collas, K. M. Kleisner, C. Longo, G. C. Osio, D. Ovando, I. Mosqueira, A. A. Rosenberg, E. R. Selig, Improving estimates of population status and trend with superensemble models. *Fish Fish.* **18**, 732–741 (2017). doi:10.1111/faf.12200

65. R. Froese, D. Pauly, FishBase; www.fishbase.org.

66. M. Palomares, D. Pauly, SeaLifeBase; www.sealifebase.org.

67. J. T. Thorson, S. B. Munch, J. M. Cope, J. Gao, Predicting life history parameters for all fishes worldwide. *Ecol. Appl.* **27**, 2262–2276 (2017). doi:10.1002/eap.1606 Medline

68. C. Boettiger, D. T. Lang, P. C. Wainwright, rfishbase: Exploring, manipulating and visualizing FishBase data from R. *J. Fish Biol.* **81**, 2030–2039 (2012). doi:10.1111/j.1095-8649.2012.03464.x Medline

69. M. N. Maunder, A. E. Punt, A review of integrated analysis in fisheries stock assessment. *Fish. Res.* **142**, 61–74 (2013). doi:10.1016/j.fishres.2012.07.025

70. R. D. Methot Jr., C. R. Wetzel, Stock synthesis: A biological and statistical framework for fish stock assessment and fishery management. *Fish. Res.* **142**, 86–99 (2013). doi:10.1016/j.fishres.2012.10.012

71. J. T. Thorson, I. J. Stewart, I. G. Taylor, A. E. Punt, Using a recruitment-linked multispecies stock assessment model to estimate common trends in recruitment for US West Coast groundfishes. *Mar. Ecol. Prog. Ser.* **483**, 245–256 (2013). doi:10.3354/meps10295